https://doi.org/10.5194/acp-2019-1070
Preprint. Discussion started: 3 December 2019

Atmospheric Chemistry and Physics Discussions

Nitrous acid (HONO) emissions under real-world driving conditions from vehicles in a UK road tunnel.

Louisa J. Kramer[1], Leigh R. Crilley[1a], Thomas J. Adams[2b], Stephen M. Ball[2], Francis D. Pope[1] and William J. Bloss[1].

[1] *School of Geography, Earth and Environmental Sciences, University of Birmingham, Birmingham, UK*

[2] *School of Chemistry, University of Leicester, Leicester, UK*

[a]*now at: Department of Chemistry, York University, Toronto, ON, Canada*

[b]*now at: Ricardo Energy & Environment, Harwell, Oxon, UK*

Correspondence to: L. J. Kramer (l.kramer@bham.ac.uk)

Abstract.

Measurements of atmospheric boundary layer nitrous acid (HONO) and nitrogen oxides (NO_x) were performed in summer 2016 inside a city centre road tunnel in Birmingham, United Kingdom. HONO and NO_x mixing ratios were strongly correlated with traffic density, with peak levels observed during the early evening rush hour as a result of traffic congestion in the tunnel. A daytime $\Delta HONO/\Delta NO_x$ ratio of 0.85% (0.72-1.01%, 95% CI) was calculated using reduced major axis regression as the overall fleet-average (comprising 59% diesel-fuelled vehicles). A comparison with previous tunnel studies and analysis on composition of the fleet suggest that goods-vehicles have a large impact on the overall HONO vehicle emissions; however, new technologies aimed at reducing exhaust emissions, particularly for diesel vehicles, may have reduced the overall direct HONO emission in the UK. This result suggests that in order to accurately represent urban atmospheric emissions and OH radical budget, fleet-weighted $HONO/NO_x$ ratios may better quantify HONO vehicle emissions in models, compared with use of a single emissions ratio for all vehicles. The contribution of the direct vehicular source of HONO to total ambient HONO concentrations is also investigated and results show that, in areas with high traffic density, vehicle exhaust emissions are likely to be the dominant HONO source to the boundary layer.

1 Introduction

Nitrous acid (HONO) is an important atmospheric constituent in the boundary layer, as its photolysis leads to the formation of OH radicals (R1), which drive atmospheric oxidation reactions, pollutant removal and the formation of secondary species. This is particularly important in urban areas where the measured HONO mixing ratios can reach up to parts per billion, and HONO photolysis can be the dominant HO_x source (Alicke et al., 2002; Elshorbany et al., 2009; Kleffmann, 2007; Lee et al., 2016; Michoud et al., 2012; Villena et al., 2011).

https://doi.org/10.5194/acp-2019-1070
Preprint. Discussion started: 3 December 2019

Atmospheric Chemistry and Physics Discussions

$$\mathbf{HONO + hv} \xrightarrow{\lambda<400\ nm} \mathbf{OH + NO} \qquad \text{(R1)}$$

The sources of HONO in the atmosphere can be primary or secondary (Figure 1). Primary sources include; direct emissions from combustion processes such as vehicle emissions (Kirchstetter et al., 1996; Liu et al., 2017; Rappengluck et al., 2013; Trinh et al., 2017; Xu et al., 2015), soil microbial activity (Laufs et al., 2017; Maljanen et al., 2013; Meusel et al., 2018; Oswald et al., 2013; Su et al., 2011) and biocrusts (Maier et al., 2018; Meusel et al., 2018; Weber et al., 2015). Secondary sources were thought to be dominated by homogeneous gas phase reaction of NO and OH during the day (resulting in a null cycle with R1), and heterogeneous production of HONO from NO_2 on surfaces at night (Calvert et al., 1994; Finlayson-Pitts et al., 2003; Jenkin et al., 1988; Kleffmann et al., 1998; Stutz et al., 2002). More recently, studies have shown that heterogeneous reactions are also important sources of HONO during the day and include photo-enhanced reduction of NO_2 on organic substrates (George et al., 2005; Monge et al., 2010; Stemmler et al., 2006) and nitrate photolysis (Reed et al., 2017; Ye et al., 2017; Zhou et al., 2011). Despite numerous studies over the last few decades, substantial uncertainties remain regarding the relative magnitude of these sources, with models frequently unable to account for total measured HONO concentrations without the inclusion of unknown sources, typically driven by photolysis (e.g. Huang et al., 2017; Lee et al., 2016; Michoud et al., 2014; Vandenboer et al., 2014; Vogel et al., 2003; Wang et al., 2017). A photo-stationary steady state method based on measurements of HONO, OH and NO_x has previously been used to infer missing HONO sources; however, in areas of high spatial heterogeneity this method breaks down because the lifetime of HONO is much longer than that of OH and NO_x (Crilley et al., 2016; Lee et al., 2013).

In areas with high traffic density, HONO emitted directly from vehicle exhausts is an important source, as indicated by large peaks in ambient HONO concentrations observed during rush hour periods (e.g. Qin et al., 2009; Rappengluck et al., 2013; Stutz et al., 2004; Tong et al., 2016; Wang et al., 2017; Xu et al., 2015). Tong et al. (2016) estimated that direct emissions from vehicles at an urban site in Beijing contributed 48.8% of the total measured HONO, almost 5 times higher than the contribution at a suburban site (10.3%) located 50 km northeast of Beijing city centre.

A $HONO/NO_x$ emission ratio is often used to parameterise the HONO contribution from vehicles. Various studies have determined this ratio either directly via chassis dynamometers (Calvert et al., 1994; Liu et al., 2017; Nakashima and Kajii, 2017; Pitts et al., 1984; Trinh et al., 2017) or from ambient roadside/tunnel measurements (Kirchstetter et al., 1996; Kurtenbach et al., 2001; Liang et al., 2017; Rappengluck et al., 2013; Yang et al., 2014). Chassis dynamometer studies benefit by the direct quantification of HONO from vehicle exhausts under different driving cycles; however, the number of vehicles included in these studies is very limited and may not be representative of the wider fleet or real world operational conditions. Both tunnel and ambient roadside measurements on the other hand allow for analysis of HONO emissions for a larger vehicle fleet, under

https://doi.org/10.5194/acp-2019-1070
Preprint. Discussion started: 3 December 2019

Atmospheric Chemistry and Physics Discussions

real-world driving conditions. Tunnel studies have the additional benefits of eliminating photolytic loss and photo-enhanced surface sources of HONO and of reducing dispersion. However, care must be taken to accurately correct for background levels of HONO at the tunnel entrance and for other HONO sources, such as heterogeneous reactions on tunnel walls and emitted particles.

Reports of the HONO/NO_x emission ratio from chassis dynamometer and ambient/tunnel studies are highly variable, ranging between 0.03 and 2.1 %, depending on fuel type and implementation of technologies aimed at reducing emissions, such as diesel oxidation catalysts (DOCs) and particulate filters (DPFs). An emission ratio of 0.8% is widely used in modelling studies, which is based on a tunnel study with a fleet comprising primarily gasoline vehicles (~75 %) conducted in 1997/98 (Kurtenbach et al., 2001). However, a recent chassis dynamometer study by Trinh et al. (2017), showed that HONO/NO_x ratios were higher from diesel vehicles (ranging from 0.16-1.00%) compared to petrol vehicles (0-0.95%), under most driving conditions. The higher HONO/NO_x ratio observed from diesel vehicle exhausts is thought to be due to a reduction-oxidation reaction as proposed by Ammann et al. (1998) and Gerecke et al. (1998) where NO_2 can be converted heterogeneously to HONO on soot via R2.

$$NO_2 + [C-H]_{red} \longrightarrow HONO + [C]_{ox} \quad \text{(R2)}$$

where, $[C-H]_{red}$ is a surface site on the soot particle.

A number of laboratory studies have supported this reaction, with HONO yields varying between 20-100 % depending on the fuel type used to generate the soot, initial NO_2 concentrations and soot coatings (Arens et al., 2001; Aubin and Abbatt, 2007; Gerecke et al., 1998; Guan et al., 2017; Khalizov et al., 2010; Kleffmann et al., 1999; Lelièvre et al., 2004; Romanias et al., 2013; Stadler and Rossi, 2000). An observation that is consistent across many laboratory experiments is that the uptake of NO_2 decreases over time, which has previously been attributed to the deactivation of soot surface receptor sites (Kalberer et al., 1999). Lelièvre et al. (2004) observed complete deactivation after the soot was exposed to ambient outdoor conditions for approximately 20 hours. As a result of the soot surface deactivation, reaction R2 is not expected to have a large impact on atmospheric HONO levels once soot has been exhausted from the vehicle. However, Khalizov et al. (2010) found that if soot was pre-heated up to 300 °C, the HONO yield increases, as a result of the removal of products from incomplete combustion, allowing for a greater number of reactive sites to reduce NO_2 to HONO. Reactions within the vehicle exhaust pipe, on fresh soot, may still be a potential source of HONO from vehicles. Determining the magnitude of this source under real-world conditions, however, is challenging. Two recent studies in Hong Kong investigated the relationship between soot and HONO directly emitted from vehicles, with contrasting results. Xu et al. (2015) found a strong positive correlation (R^2 = 0.83) between HONO/NO_x and black carbon (BC) in fresh traffic plumes sampled at an ambient air monitoring site, but no correlation was ascertained in a separate road tunnel experiment by Liang et al. (2017). Data taken at a site in North Kensington, London,

https://doi.org/10.5194/acp-2019-1070
Preprint. Discussion started: 3 December 2019

Atmospheric Chemistry and Physics Discussions

during 2012 as part of the Clean Air for London (ClearfLo) project show a correlation between HONO and BC (R^2=0.71); however, there is no clear correlation between HONO/NO_x and BC when sampling fresh pollution plumes (i.e. when NO/NO_x ratios are large) (see Figure S1 in the supplementary material). This agrees with Liang et al. (2017) who suggested that HONO formed via NO_2 conversion on BC may be insignificant even in a road tunnel scenario shortly after emission.

The primary aim of this study is to determine HONO/NO_x emission ratios under real-world driving conditions, with a fleet containing a high proportion of diesel vehicles. In the UK, at the end of 2016, there were over 38 million vehicles licensed for use on the roads (DfT, 2017). The majority of licensed vehicles were passenger cars (~83%) and goods vehicles (11.4%), with the remainder consisting of motorcycles, buses/coaches and other vehicles (e.g. agricultural machines, ambulances). Diesel fuelled cars and goods vehicles, in total, account for 44% of the vehicles on the road in the UK in 2016 (data on the statistics discussed here can be found in Table S1 in the supplementary material). To our knowledge this is the first study of direct HONO exhaust emissions performed in the UK and the first study in any country that has a diesel composition greater than 40% of the vehicle fleet. Using co-located HONO, NO_x and CO_2 data, we investigated the HONO/NO_x ratio using measurements taken in a road-tunnel in the city centre of Birmingham and considered the impact of new technologies implemented in the European emission standards on the measured HONO emissions. Finally, the contribution of direct HONO emissions to the total HONO measured in an urban area was determined.

2 Experimental

2.1 Queensway Tunnel

Measurements took place in the southbound bore of the Queensway Tunnel (Figure 2), a two-bore, twin lane tunnel, 548 m in length located in the centre of Birmingham, UK (52° 28' 46" N, 1° 54' 20" W). The tunnel forms part of the A38 roadway which is a major route in to and out of Birmingham City Centre, and links to the M6 motorway north of the city. The instruments were located at the distant end of a maintenance area approximately 435 m from the entrance to the southbound tunnel. The two bores of the tunnel are separated by a solid wall eliminating any influence in the measurements from vehicles travelling in the northbound bore. The tunnel was not mechanically ventilated during the measurement period. Airflow through the tunnel therefore is via natural wind flow or induced by vehicle movement (piston effect). The average speed of vehicles through the tunnel during the daytime (06:00-19:59) is 52 kph (33 mph) which drops to 33 kph (21 mph) at 17:00 during peak evening rush hour as a result of congestion (see Figure S2).

2.2 Fleet information

Data from an Automatic Number Plate Recognition (ANPR) camera commissioned by Birmingham City Council were used to obtain information on the vehicle fleet passing through the tunnel. ANPR data were taken from 8-11 November 2016 and

https://doi.org/10.5194/acp-2019-1070
Preprint. Discussion started: 3 December 2019

included vehicle type, euro classification and capture rate of the vehicle number plates, on a 15 minute time scale. The ANPR capture rate is based on a comparison of manual classified counts (MCC) with the ANPR data. The capture rate was typically around 90% of MCC, with counts missing from ANPR usually as a result of the number plate being obscured (Rhead et al., 2012). We assumed the same fleet proportions for the missing vehicle counts and adjusted the final data accordingly. Figure 3 shows the mean hourly number of vehicles travelling through the tunnel during the weekdays and breakdown of vehicles by type. The ANPR data were compared to manual traffic counts performed at the exit of the southbound tunnel on selected days during the measurement period with good agreement. Approximately 37,700 vehicles travel through the southbound bore of the Queensway tunnel during an average weekday. The majority of these vehicles are petrol (40%) and diesel (44%) fuelled passenger cars, with the remaining fleet comprised primarily of diesel fuelled light-goods vehicles (LGVs, e.g. vans, small pick-ups) (10.4%), ordinary goods vehicles (OGVs, e.g. trucks, articulated vehicles) (2.5%) and passenger vehicles (taxis and buses) (1.3%).

2.3 Instrumental techniques

The instruments were installed in the tunnel in close proximity (1.5 m) to the roadside and made measurements from 29th July until 8th August 2016. Access to the instruments was only possible when the tunnel was closed to traffic during maintenance periods, which occurred approximately every 2 weeks. Table 1 provides an overview of the instrumentation deployed in the tunnel during the campaign.

Direct spectroscopic measurements of HONO and NO_2 were made by broadband cavity enhanced absorption spectroscopy (BBCEAS) (Langridge et al., 2009; Thalman et al., 2015). The BBCEAS instrument operated in the wavelength range 363–388 nm, which includes a highly structured part of the NO_2 spectrum and two HONO absorption bands at 368 and 385 nm. Ultraviolet light from an LED light source was directed through a cavity formed by two highly reflective mirrors (99.94%) separated by 80 cm, giving an effective path length of approximately 1.4 km. The mirrors were housed in bespoke mirror mounts (length = 11 cm) which were purged with nitrogen (0.9 L/min divided between the two mounts), and thus BBCEAS data were corrected for the cavity's length factor (LF = 1.37). The cavity was operated "open path", i.e. the portion of the cavity between the mirror mounts was open to the ambient atmosphere. This open path configuration has the advantage that there were no wall losses or heterogeneous production of HONO within the instrument. In the field, a Teflon tube was inserted between the mirror mounts in order to measure the reference spectrum of light transmitted when the cavity was purged with nitrogen. The reflectivity of the cavity mirrors (as a function of wavelength) was characterised in the laboratory before the

https://doi.org/10.5194/acp-2019-1070
Preprint. Discussion started: 3 December 2019

Atmospheric Chemistry and Physics Discussions

campaign. The reflectivity was verified in the field by measuring the 380 nm absorption band of O_4 when purging the cavity with pure oxygen, and measurements taken at the start and end of the campaign agreed to within 4.5%.

BBCEAS spectra were integrated for 20 s (the average of two 10 s acquisitions). Spectra fitted with reference absorption cross sections for HONO (Stutz et al., 2000), NO_2 (Vandaele et al., 1998) and O_4 (Hermans as given in the HITRAN database, Richard et al., 2012), and any remaining unfitted broadband absorption was attributed to extinction by ambient aerosol particles. Typical statistical errors for retrieving HONO and NO_2 concentrations from the spectral structure were 0.8 ppbv and 0.9 ppbv, respectively. The BBCEAS measurements are also affected by systematic uncertainties in the reference absorption cross sections (typically 3%) and for determining the mirror reflectivity in the field (4.5%). Extinction by ambient aerosol also reduced the effective path length of the BBCEAS measurement. HONO retrievals tended to be dominated by statistical (spectral fitting) errors, whereas retrievals of the much high ambient NO_2 concentrations were dominated by the systematic uncertainties. For the mean HONO (3 ppbv) and NO_2 (75 ppbv) amounts recorded during the campaign, the total measurement uncertainties were 1.2 ppbv for HONO and 5 ppbv for NO_2.

NO was measured by a commercial chemiluminescence NO_x analyser (Thermo Environmental Instruments Inc: Model 42C). The detection limit of the 42C was determined from 3 times the standard deviation of the measurement in zero air and was calculated to be approximately 0.2 pbbv for a 1 minute averaging period. The uncertainty of the instrument was estimated to be 10% from calibrations. The analyser is capable of measuring NO_2 and NO_x, however the instrument utilises a molybdenum converter to covert NO_2 to NO, an approach which is known to be influenced by positive interference from other NO_y species such as HONO, nitric acid (HNO_3), peroxyacetyl nitrate (PAN), and alkyl nitrates (e.g. Dunlea et al., 2007; Villena et al., 2012); therefore the final NO_x used in this study is calculated from the sum of the NO measured by the 42C and NO_2 by the BBCEAS. The inlet for the 42C instrument was shared with a non-dispersive infrared instrument (LI-COR: Model LI-820) to measure CO_2. The LI-COR was calibrated with pure N_2 (0 ppmv CO_2) and 1500 ppmv CO_2 to determine the relative uncertainty (5%) and precision (1.2 %, 2-σ). The LI-COR and 42C analysers were evaluated for drift from zero measurements taken before and after the measurement campaign. The drift for CO_2 and NO_x were determined to be 1.45 ppmv and 0.42 ppbv, respectively. The drift for both instruments was less than 2% of the minimum measured values in the tunnel (NO = 1.27%, CO_2 = 0.35%), therefore no correction was deemed necessary here. A mini-met station/anemometer (Kestrel 4500) was deployed near the top of the tunnel (3m above ground level and 1m from road side) to measure the temperature, relative humidity and air flow in the tunnel.

https://doi.org/10.5194/acp-2019-1070
Preprint. Discussion started: 3 December 2019

Atmospheric Chemistry and Physics Discussions

3 Results and discussion

3.1. Data Overview

Figure 4 presents 15-minute averaged time series for gases measured in the tunnel. HONO, NO_2 and CO_2 follow the same diurnal cycle indicating that they have a similar source. There is a clear difference in weekday and weekend diurnal cycles with peaks associated with rush hour traffic observed in NO_x, HONO and CO_2 during the weekdays, which are not present at the weekend. NO_x, HONO and CO_2 concentrations are also lower at the weekend. The mixing ratios of all gas species during weekdays increase from around 06:00 (start of morning rush hour) and drop away in the afternoon. A large spike in the evening around 17:30 – 18:00 is observed, which coincides with congestion in the southbound tunnel during peak evening rush hour.

The mean weekday HONO mixing ratio during the daytime (06:00 to 19:59, calculated from the 15 minute averages) is 3.4 ±1.0 ppbv (1-σ), which decreased to 2.4 ± 0.7 ppbv overnight. The maximum observed 15 minute average HONO level occurred during the evening rush hour, reaching 9.7 ppbv on 3rd August. Observed HONO levels in the current work are typically lower than in previous tunnel studies. Liang et al. (2017) measured a mean HONO level of 15.7 ± 4.2 ppbv during their study in Hong Kong, whereas Kurtenbach et al. (2001) observed peak HONO levels of 45 ppbv in the daytime. Kirchstetter et al. (1999) only performed measurements between 16:00 to 18:00 in the Caldecott Tunnel, California and observed a mean HONO level of 6.9 ± 1.4 ppbv, higher than the mean level of 4.1 ± 1.4 ppbv for the same hours in this study. The lower levels measured in the current study may be the result of differences in vehicle fleet between studies as discussed further in Section 3.3, in combination with shorter tunnel length (Table 2) and shorter distance of the sampling point into the tunnel.

The persistence of HONO overnight is unlikely to be due to vehicle exhaust emissions as traffic is low during this period, but rather from background ambient HONO entering at the tunnel's entrance and heterogeneous formation of HONO on the walls of the tunnel (Kurtenbach et al., 2001). This suggests that vehicles were not the only source of HONO during the day and the impact of heterogeneous HONO formation is considered in emission ratio calculations in Section 3.2.1.

From late evening on 1st August until mid-morning on 2nd August the HONO mixing ratios are lower than otherwise observed for a weekday. Precipitation data from a nearby weather station (Figure S3) revealed that it rained continuously from 17:00 on 1st August to 16:00 on 2nd August with corresponding high relative humidity recorded inside the tunnel. It is likely that wet surfaces inside the tunnel, as a result of spray from tyres, resulted in a loss in HONO. The Henry's law constant (in water) of HONO ($k_H = 4.8 \times 10^{-1}$ mol m^{-3} Pa^{-1}) is approximately 4800 times greater than that of NO_2 ($k_H = 9.9 \times 10^{-5}$ mol m^{-3} Pa^{-1}) (Sander, 2015), therefore HONO is likely to be washed out more rapidly than NO_2 on wet surfaces, resulting in a deviation in

https://doi.org/10.5194/acp-2019-1070
Preprint. Discussion started: 3 December 2019

Atmospheric Chemistry and Physics Discussions

the HONO/NO_x ratios. As a result, this precipitation event was excluded from the final dataset for calculation of emission ratios.

3.2 Relative HONO emission ratios

To determine a HONO/NO_x emission ratio representative of direct exhaust emissions, correction for both heterogeneous formation of HONO from NO_2 and background HONO levels were considered.

3.2.1 Heterogeneous HONO formation from NO_2

A number of heterogeneous reactions resulting in the formation of HONO have been proposed in the literature, however, the formation of HONO from NO_2 on humid surfaces (R3) is thought to be the main pathway (Spataro and Ianniello, 2014 and references therein).

$$2\,NO_{2(g)} + H_2O_{(ads)} \rightarrow HONO_{(g)} + HNO_{3(g)} \qquad \text{(R3)}$$

The rate of reaction R3 (k_{het}) is dependent on the geometric uptake coefficient of NO_2 on the tunnel walls (γ_{geo}) and given by:

$$k_{het} = \frac{1}{8}\bar{v}_{NO2}\frac{S}{V}\gamma_{geo}, \qquad \text{(Eq. 1)}$$

where $\bar{v}_{NO2}$ is the mean molecular velocity of NO_2 and *S/V* is the surface-to-volume ratio of the tunnel (Kurtenbach et al., 2001). Kurtenbach et al. (2001) performed laboratory experiments to measure HONO generated on tunnel wall residue to directly calculate γ_{geo} and determined $k_{het} = 3 \times 10^{-3}$ min^{-1}.

The rate of formation of HONO from NO_2 can then be calculated via Eq. 2.

$$\frac{d[HONO]}{dt} = -\frac{1}{2}\frac{d[NO_2]}{dt} = k_{het}[NO_2] \qquad \text{(Eq. 2)}$$

where *dt* is the residence time of the gases in the tunnel from the entrance to the sampling point.

Kurtenbach et al. (2001) calculated that the heterogeneous conversion on the tunnel wall contributed to approximately 13% of the measured HONO during the day and up to 80% at night (for a maximum NO_2 mixing ratio of 250 ppbv). This result is in

https://doi.org/10.5194/acp-2019-1070
Preprint. Discussion started: 3 December 2019

Atmospheric Chemistry and Physics Discussions

contrast to measurements obtained in the Caldecott Tunnel by Kirchstetter et al. (1996) who showed that the $HONO/NO_x$ ratio did not change between the middle of the tunnel and the tunnel exit, suggesting that there was no significant formation of HONO (or deposition of HONO) on the tunnel walls in their study.

Liang et al. (2017) determined $k_{het} = 1.31 \times 10^{-3}$ min^{-1} in the Shing Mun tunnel, Hong Kong from using an upper limit of $\gamma_{geo} = 10^{-6}$ as calculated by Kurtenbach et al. (2001). Using wind speed data in the tunnel to determine the residence time, Liang et al. found on average that the contribution of $HONO/NO_x$ from heterogeneous reactions on the tunnel walls alone was 0.04%. Since this value was less than the error when calculating $HONO/NO_x$ from direct emissions, the authors did not perform any corrections to the final $HONO/NO_x$ ratio. As there is no consensus in the literature to the relative contribution from tunnel walls to measured HONO, we calculated the contribution from heterogeneous HONO formation in the Queensway tunnel during the measurement period. Using Eq. 1, a geometric uptake coefficient for NO_2 of $\gamma_{geo} = 10^{-6}$ and the surface-to-volume ratio of the Queensway tunnel (0.64 m^{-1}), we calculated k_{het} to be 1.9×10^{-3} min^{-1}.

The Kestrel anemometer used in this study logged data every 20 minutes, and as a result, the wind speed measurements inside the tunnel only provide a "snap-shot" of the data and are dependent on the traffic flow. Care should be taken when using wind speed measured by an anemometer to calculate the air's residence time in a tunnel. Rogak et al. (1998) compared residence times in a tunnel calculated using an SF_6 tracer and anemometer data and found that the wind speed in the tunnel measured by the anemometer overestimates volumetric flow during high wind speeds and underestimates when wind speed is low, requiring a correction factor for the determination of emission factors in the tunnel. Tracer measurements were not performed during our study, consequently a modelling approach was used to correct the wind speed data from the anemometer. As outlined below the wall source contribution to the observed HONO was small (~5% on average) during the daytime periods used to derive our final results.

"True" wind speeds were inferred from computational fluid dynamics (CFD) modelling of CO_2 profiles measured along the tunnel. After the campaign, the LI-COR CO_2 instrument was installed into a van and driven repeatedly through the south-bound bore of the tunnel at four different times of the day (late morning, late afternoon, evening and at night). Data recorded when the van was inside the tunnel were extracted from the CO_2 time series. The timestamps of these data points were converted into distance along the tunnel using the speed of the van and the time that it entered the tunnel, as recorded by a camera mounted on the van's dashboard. The CO_2 data were then averaged into 50 m bins along the tunnel to produce a profile of the CO_2 concentration increasing with distance into the tunnel. The CO_2 profiles were simulated by a CFD model which took as its inputs the tunnel's physical dimensions, the anemometer wind speed, the ANPR traffic counts and traffic composition, and emission factors from the DEFRA Emissions Factor Toolkit version (EFT v8.0.1) (DEFRA, 2017). Further information on the DEFRA EFT is provided in the supplementary material. The wind speeds that produced the optimum fits

https://doi.org/10.5194/acp-2019-1070
Preprint. Discussion started: 3 December 2019

Atmospheric Chemistry and Physics Discussions

between modelled and measured CO_2 profiles are shown as the crosses in Figure S4. These wind speeds match closely with the anemometer wind speeds increased by a factor of 3.0 and they correctly capture the day and night-time differences. The optimum CFD-inferred wind speeds at 10:00, 16:00 and 20:00 (3.4 to 3.9 m s^{-1}) are also in agreement with the 3.6 m s^{-1}wind speed (06:00 to 23:59) in the tunnel study by Liang et al. (2017); and consistent with the empirical correction factor produced by Rogak et al. (1998) of ×3.5 for an anemometer-measured wind speed of 1.5 m s^{-1} applicable during much of the daytime. The results of CFD modelling of CO_2, NO_2 and HONO profiles measured in the Queensway tunnel will be published in a separate paper.

During the night, the measured wind speed was often below the minimum speed required to turn the anemometer's impeller (< 0.4 m s^{-1}) so the residence time of the air parcel overnight is difficult to determine directly. As a result, we focus here on the heterogeneous formation of HONO in the tunnel during the daytime (see comments below, in Section 3.2.3, regarding use of daytime only data to infer the fleet average emission ratios). Between 06:00 and 19:59 the mean wind speed in the tunnel was 3.89 m s^{-1}, giving a residence time of air in the tunnel up to it reaching the sampling point of 1.86 minutes. If we assume the mean residence time of NO_2 emissions in the tunnel is half of this residence time (Liang et al., 2017; Pierson et al., 1978), the HONO produced from heterogeneous formation on the tunnel walls is 0.18 ppbv for a mean daily weekday NO_2 mixing ratio of 98 ppbv, which is approximately 5% of the mean measured HONO in the day. Although the mean heterogeneous contribution to HONO during the daytime is small, the heterogeneous contribution is higher (8%) when the tunnel becomes congested and the residence time of the air in the tunnel increases. Therefore, the final HONO data used in this study was corrected for the heterogeneous HONO contribution using measured NO_2 and the modelled wind speed, to better represent the direct HONO emissions in the tunnel.

3.2.2 Background corrections for HONO, NO_x and CO_2

As vehicles travel through the tunnel, cleaner air from outside is drawn into the tunnel diluting the vehicle emissions, known as the piston effect. To obtain direct vehicle emission measurements it is necessary to correct for the dilution by subtracting ambient background levels from the concentrations measured in the tunnel. As no concurrent measurements were available at the tunnel entrance during this campaign, ambient NO_x, HONO and CO_2 data from nearby stations were used to correct for the background levels. Hourly averaged background NO_x mixing ratios during the measurement period were taken from Acocks Green (AG), an Automatic Urban Rural Network (AURN) site located 6.9 km south east of the Queensway Tunnel (http://uk-air. defra.gov.uk/). The AURN station does not measure HONO or CO_2, so data previously taken at the Birmingham Air Quality Supersite (BAQS) on the University of Birmingham campus (52° 27' 1" N, 1° 55' 30" W) 3 km south west of the tunnel

https://doi.org/10.5194/acp-2019-1070
Preprint. Discussion started: 3 December 2019

Atmospheric Chemistry and Physics Discussions

was used in this study. As CO_2 is well mixed within the troposphere, variability in background CO_2 mixing ratios levels is primarily the result of a changing boundary layer height. Therefore, in this study, an average diurnal CO_2 cycle measured at BAQS was used to correct for background. The overnight background corrected CO_2 ($\Delta CO_2 = CO_{2.tunnel} - CO_{2.bkg}$) levels dropped to near zero (see panel C of Figure 5) suggesting that the procedure was suitable. HONO on the other hand has a much shorter lifetime than CO_2 and HONO mixing ratios vary depending on local sources and availability of NO_2 (Crilley et al., 2016). An average diurnal HONO/NO_x cycle (Figure S5) was calculated from measurements taken at BAQS between 18th March and 1st April, 2015 (Singh, 2017) and applied to the background NO_x from Acocks Green to determine hourly background HONO mixing ratios (Eq 3).

$$[\mathrm{HONO}]_{\mathrm{bkg}} = [\mathrm{NOx}]_{\mathrm{bkg(AG)}} \times \left(\frac{[\mathrm{HONO}]}{[\mathrm{NOx}]}\right)_{\mathrm{BAQS}} \quad \text{(Eq. 3)}$$

Figure 5 shows the hourly time series of NO_x, HONO and CO_2 measured in the tunnel and the corresponding data corrected for background mixing ratios. The results show that mixing ratios measured in the tunnel were, on average, 73 and 44 times higher than the background NO_x and HONO, respectively, suggesting that direct emissions from vehicles were indeed the dominant source of these gases. Consequently, any uncertainties in the background HONO mixing ratios that were subtracted from the measured HONO have little impact on the final results.

3.2.3 HONO emission ratios

To determine the HONO to NO_x emission ratio, a reduced-major-axis (RMA) regression (Figure 6) was performed using the weekday hourly averaged data from 06:00 to 19:00, i.e. when there was minimal contribution from heterogeneous HONO sources and the traffic flow was high (> 1500 vehicles per hour). The slope of the regression gives an average emission ratio of $\Delta HONO/\Delta NO_x$ = 0.85 % (95% confidence interval = 0.72-1.01 %) for this time period.

Figure 7a shows that the $\Delta HONO/\Delta NO_x$ emission ratio varies during the day, from 0.66% at 07:00 to 1.10% at 19:00. In this section, we explore the relationship between $\Delta HONO/\Delta NO_x$ and changes in vehicle fleet composition using information on fuel and vehicle type from the ANPR dataset. Figure 7c shows the fraction of diesel and non-diesel (petrol, LPG and electric) vehicles travelling through the Queensway tunnel during an average weekday. Between 06:00 and 17:00, the $\Delta HONO/\Delta NO_x$ ratio appears to vary closely with changes in the fraction of diesel vehicles, with both variables peaking at 10:00 when the $\Delta HONO/\Delta NO_x$ emission ratio reaches a value of 0.91% and the percentage of diesel fuelled vehicles in the fleet reaches a maximum of 66%.

https://doi.org/10.5194/acp-2019-1070
Preprint. Discussion started: 3 December 2019

Atmospheric Chemistry and Physics Discussions

The $\Delta HONO/\Delta CO_2$ ratio (Figure 7b and Table S2) also follows the change in fleet composition, with a higher ratio observed at 10:00 (3.3%) compared to 17:00 (1.5%). However this may also be the result of higher CO_2 emissions from petrol fuelled vehicles compared to diesel vehicles; for example, a study of 149 passengers cars showed that CO_2 emissions were 13–66% higher for petrol vehicles than diesel (O'Driscoll et al., 2018). Modelled emission factors from the DEFRA Emissions Factors Toolkit (EFT v8.0.1) indicate a maximum in the CO_2 emissions (mg veh^{-1} km^{-1}) at 17:00 (Figure S6), in line with the 46% maximum in the non-diesel vehicle fraction at evening rush hour.

From 17:00 to 19:00 the relationship between the ΔHONO ratios and fuel type is less clear. During this period the fraction of diesel vehicles remains almost constant, however, the $\Delta HONO/\Delta NO_x$ and $\Delta HONO/\Delta CO_2$ emission ratios both sharply increase. Analysis of the modelled NO_x and CO_2 emission factors from the EFT (Figure S6) indicate a decrease in both NO_x and CO_2 emission factors from 17:00 to 19:00, which is likely to be related to the total vehicle flow and vehicle speed (because the fleet composition remains very similar). The EFT does not have the capability to determine a HONO emission factor, therefore information on HONO emission variability with speed and vehicle flow is not available. However, assuming the HONO emissions do not reduce by the same percentage after 17:00, this would lead to the increase in the observed $\Delta HONO/\Delta NO_x$ and $\Delta HONO/\Delta CO_2$ ratios. As no conclusion can be made at this point, without additional information, we focus the analysis in the following section on the data between 06:00 and 17:00.

Ho et al. (2007) used equation 4 to determine emission factors (mg veh^{-1} km^{-1}) for diesel and non-diesel fuelled vehicles based on a method described by Pierson et al. (1996).

$$EF = (EF_{DV} - EF_{NDV})x + EF_{NDV} \qquad \text{(Eq. 4)}$$

where, x is the fraction of diesel-fuelled vehicles, EF_{DV} is the emission factor for diesel vehicles, EF_{NDV} the emission factor for non-diesel vehicles and EF is the emission factor for the mixed fleet. In this format, a linear regression of x versus EF, based on equation 4, gives EF_{DV} at $x = 1$ and EF_{NDV} at $x = 0$.

In this study, instead of calculating emission factors, we investigated application of equation 4 to determine $\Delta HONO/\Delta NO_x$ emission ratios for diesel (ER_{DV}) and non-diesel (ER_{NDV}) vehicles (see Figure S7). However, this method resulted in an unrealistic small negative emission ratio for non-diesel vehicles (ER_{NDV} = -0.01%). This method may not be appropriate for the current work because the range in the fuel fraction of vehicles is small, thus extrapolating to $x = 0$ and $x = 1$ resulted in very large uncertainties.

https://doi.org/10.5194/acp-2019-1070
Preprint. Discussion started: 3 December 2019

Atmospheric Chemistry and Physics Discussions

An alternative approach is to determine emission ratios using a pair of simultaneous equations based on the fraction of diesel vehicles and $\Delta HONO/\Delta NO_x$ values for different hours of the day. For example, using the data as given in Table S2, the equation at 17:00 is given by:

$$\frac{\Delta HONO}{\Delta NOx} = 0.73\% = 0.54 \times ER_{DV} + 0.46 \times ER_{NDV} \qquad \text{(Eq. 5)}$$

Using the equation for a different hour (i.e. different set of fractions), the values for ER_{DV} and ER_{NDV} can be determined. Care must be taken when interpreting these results, however, as the calculated ERs depend on the selection of pairs of measurement points and some pairs resulted in negative ER values. Thus average ERs were determined using many pairs of simultaneous equations. Here we calculated the average of ten ERs, using one set of fractions at 17:00 and a second set for each hour from 06:00 to 15:00. The data from 16:00 was not used here as there was no change in the diesel fraction between 16:00 and 17:00. The mean (± 1σ) for ER_{DV} and ER_{NDV} are 1.66 ± 2.2 % and 0.4 ± 0.5 %, respectively, suggesting that diesel fuelled vehicles do have higher $\Delta HONO/\Delta NO_x$ ratios.

It has previously been suggested that higher $HONO/NO_x$ ratios are observed when the tunnel fleet contains a greater number of heavy duty vehicles (Trinh et al., 2017). A similar calculation to that outlined in the previous paragraph was performed to determine the average emission ratio for cars and for heavy duty vehicles (goods vehicles and buses) by apportioning the observed $\Delta HONO/\Delta NO_x$ ratios between the car and heavy duty vehicle numbers given in Table S2. The $\Delta HONO/\Delta NO_x$ ratio emission ratio for heavy duty vehicles (ER_{HD}) is estimated to be 1.28 ± 0.64%, approximately 1.9 times higher than the ratio determined for cars (ER_{CAR} = 0.69 ± 0.05%). The impact of heavy duty vehicles on the $HONO/NO_x$ emission ratio is discussed further in section 3.3.

It should be noted that the methods described above can only provide an estimate of the emission ratios for different fuel and vehicle types. In our study, the variability in the fraction of diesel vehicles and heavy duty vehicles across the day was small, therefore extracting emission ratios for individual vehicle types is challenging. To obtain more precise emission ratios for different engine types, a larger dataset (i.e. longer time series) and contemporaneous ANPR data would be required.

3.3 Comparison of $HONO/NO_x$ emission ratios across tunnel studies

Table 2 shows a comparison of measured $HONO/NO_x$ emission ratios for studies performed in road tunnels, along with summaries of their reported vehicle fleets. The lowest $HONO/NO_x$ ratio (0.29%) was measured in the Caldecott tunnel, California (Kirchstetter et al., 1996). As 99% of the fleet was comprised of petrol fuelled vehicles, the low $HONO/NO_x$ ratio

https://doi.org/10.5194/acp-2019-1070
Preprint. Discussion started: 3 December 2019

is expected because the analysis in section 3.2.3 and dynamometer studies have demonstrated that petrol vehicles typically emit less HONO than diesel. On the other hand, Liang et al. (2017) observed a HONO/NO_x emission ratio of 1.24 ± 0.35 % in the Shing Mun Tunnel, Hong Kong in 2015, approximately 1.4 times higher than in the current work despite the Queensway Tunnel having a higher proportion of diesel vehicles compared to the Shing Mun Tunnel (59% and 38% respectively). The differences observed in the HONO/NO_x emission ratio between the Shing Mun and Queensway tunnel studies may be related to 1) the percentage of heavy duty & goods vehicles within the fleet, and 2) after treatment technologies that affect NO_2 emitted directly from vehicle exhausts (known as primary NO_2).

In addition to these two points, which are discussed further below, it should also be noted that the fleet in the Shing Mun Tunnel consisted of 15% liquefied petroleum gas (LPG) fuelled vehicles. On road sampling of emissions from buses fuelled by diesel and LPG in Hong Kong have indicated that LPG vehicles have lower NO_x emissions when compared to diesel (Ning et al., 2012). However, as far as we are aware there have been no published studies investigating HONO emissions from LPG fuelled vehicles, and therefore no conclusions can be made at this point regarding the impact of the LPG fleet on the observed differences in HONO/NO_x ratios.

Liang et al. (2017) investigated the impact of diesel particle filters (DPFs) on HONO vehicle emissions and found that HONO emissions ratios were higher in vehicles equipped with DPFs (based on a higher $\Delta NO_2/\Delta NO_x$ ratio) and suggest that this may be due to HONO formation from heterogeneous reactions involving NO_2 and black carbon within the filter. The diesel oxidation catalysts (DOCs) oxidise hydrocarbons and CO in excess oxygen over platinum/palladium catalysts; however NO can also be oxidized to NO_2 during this process. DPFs were mandatory for all new diesel vehicles from 2009 (Euro Class V) and operate by trapping soot in the exhaust where it is then oxidized at high temperatures. To ensure the filters do not become blocked from engines that run at lower temperatures, many DPFs use catalysts to convert NO to NO_2 to periodically oxidise the soot (He et al., 2015; Kim et al., 2010). Consequently, DOCs and DPFs both result in an increase in NO_2 emitted from exhausts, which may also lead to an increase in HONO emissions.

Liang et al. estimated that half of the diesel fleet in their study were buses and goods vehicles (Euro Class IV and above) equipped with diesel particulate filters. In the current work less than a quarter of diesel fuelled vehicles were goods vehicles or buses, and of those only 58% were Euro Class V and above (i.e. with DPFs fitted). As a result, the percentage of diesel vehicles emitting high NO_x and HONO levels is expected to be much lower in the Queensway tunnel than the Shing Mun tunnel, and this likely accounts for the lower HONO/NO_x emission ratio we observed. In contrast in the Kiesbergtunnel (Kurtenbach et al., 2001), medium and heavy-duty vehicles represented 12% of the fleet (6% heavy-duty trucks, 6% commercial vans), similar to the fleet in the Queensway tunnel, which may explain why the observed HONO/NO_x emission ratios were so similar (0.85% and 0.8%, for the Queensway tunnel and Kiesbergtunnel studies, respectively). It should be

https://doi.org/10.5194/acp-2019-1070
Preprint. Discussion started: 3 December 2019

noted that the Kiesbergtunnel fleet were all pre-Euro III standard, so higher emissions of NO_x are expected compared to later Euro standard vehicle classes. However, few of these vehicles in the Kiesbergtunnel would have been fitted with DOCs or DPFs, so this may have offset the amount of NO_2 (and thus HONO) emitted.

Recent trend analysis studies have shown that primary NO_2 has been decreasing over the last decade in the UK (Carslaw et al., 2016; Matthaios et al., 2018) and across Europe (Grange et al., 2017). For example, the mean NO_2/NO_x emission ratio measured from ambient roadside monitoring sites in inner-London has decreased from a peak value of 25% in 2009 to 15% in 2014 (Carslaw et al., 2016). Although the exact cause of the NO_2 reduction is not clear, it is thought that the introduction of after-treatment technologies, such as selective catalytic reduction (SCR) installed on buses and heavy duty vehicles, and a reduction in the use of platinum group metals in catalysts may contribute to the observed decrease (Carslaw et al., 2016; Grange et al., 2017). With a reduction in NO_2 emissions from diesel vehicles overall, a decrease in HONO may also be expected in the UK. In contrast, Wang et al., (2018) reported an increase in the NO_2/NO_x ratio at the outlet of the Shing Mun tunnel, from 9.5% in 2003 to 16.3% in 2015. Therefore the higher $HONO/NO_x$ ratio observed in Hong Kong (Liang et al. (2017)) compared to current work may also be related to differences in primary NO_2 emissions. It should be noted that in the study by Wang et al., NO_2 was measured using a standard chemiluminescence monitor, which typically use a molybdenum converter. Molybdenum converters also convert other NO_y species, such as HONO, resulting in an overestimation of the reported NO_2. However, as the $HONO/NO_x$ ratio was only 1.24%, it is unlikely that HONO has contributed to the factor of 1.7 increase in primary NO_2 recorded near the Shin Mung Tunnel.

4 Impact of HONO emissions from vehicles on total HONO measured in Birmingham.

Previous work has shown that ambient HONO has large heterogeneity when sampling close to roads (Crilley et al. 2016). Here we use the mean $HONO/NO_x$ emission factor of 0.85%, determined from the tunnel measurements in section 3.2.3, to investigate the contribution of direct HONO vehicle emissions to ambient HONO levels in urban and suburban areas. Measurements of HONO and NO_x were taken in a mobile laboratory on a return journey between Birmingham and Leicester, two cities in the UK Midlands separated by 55 km (straight line measurement from city centres). NO and NO_2 were measured every 60 s by a chemiluminescence analyser fitted with a molybdenum NO_2 converter (Thermo 42i-TL). As discussed in section 2.3, molybdenum converters are known to result in interferences from NO_y species, therefore the NO_x measurements presented here represent an upper limit on $NO + NO_2$. HONO was measured every 5 minutes with a Long-Path Absorption Photometer (LOPAP, Model 03, QUMA). Measurement uncertainties are primarily the result of uncertainties in the calibrations and are estimated to be 5% and 10%, for NO_x and HONO, respectively. Further details regarding the measurement techniques and the driving route can be found in Crilley et al. (2016).

https://doi.org/10.5194/acp-2019-1070
Preprint. Discussion started: 3 December 2019

Atmospheric Chemistry and Physics Discussions

Figure 8 shows measured HONO and NO_x mixing ratios during the transect from Birmingham to Leicester and the return journey, on 23 October 2015. Also shown is the directly emitted vehicular HONO ($HONO_{veh}$) calculated from the mean $\Delta HONO/\Delta NO_x$ emission ratio (0.85%). For the two transects, $HONO_{veh}$ contributed on average 66% to the total measured HONO. The highest contribution was observed on the M6 motorway, where $HONO_{veh}$ typically accounted for 86% of the measured HONO. During the motorway segments of the journeys, the mobile laboratory was operating in "chase mode", i.e. deliberately sampling plumes from a single vehicle ahead. Therefore, it was likely the high $HONO_{veh}/HONO$ ratios observed on the motorway were the result of predominantly sampling vehicle emission plumes with low background contribution. The lowest $HONO_{veh}$ contribution was observed around the Birmingham University campus (24%), which is expected as traffic density was low in this area. Whilst travelling through Birmingham city centre, $HONO_{veh}/HONO$ increased to 70%, indicating that vehicle exhaust emissions were the dominant source of HONO in this area. This value is higher than determined by Tong et al. (2016) in Beijing (48%); however, in our study we were sampling directly on the road, whereas the site in Beijing was located in a building at the Institute of Chemistry, Chinese Academy of Sciences, therefore significantly less influenced by direct traffic sources. This estimate neglects the differing atmospheric lifetimes of HONO and NO_x; the longer lifetime of the latter implies that $HONO/NO_x$ ratios will fall as the airmass ages. Accordingly, estimates of the vehicular contribution derived from measurements made as close as possible to the emission source, i.e. on the roadway, as described here, will give the lowest estimate of the relative importance of vehicle emissions.

Overall direct vehicle emissions can be an important source of HONO in urban areas, particularly near roads with very high traffic density. Further investigation in these areas is paramount to fully understand the impact of OH produced from HONO on chemical processing in the overlying atmosphere.

5 Summary

Measurements of HONO, NO_x and CO_2 were performed in a city centre road tunnel in Birmingham, UK for two weeks in July/August 2016, to investigate direct HONO emissions from vehicle exhausts under real-world driving conditions. HONO mixing ratios peaked when NO_x and CO_2 peaked during traffic congestion in the weekday evening rush hours (17:30 – 18:00), confirming that vehicle exhausts were the dominant source of HONO in the tunnel.

A $HONO/NO_x$ emission ratio of 0.85% (0.72-1.01%, 95% CI) was determined for an average weekday fleet comprising 59% diesel fuelled vehicles. Our value is similar to the ratio of 0.8% which is typically used in modelling studies and which was determined for a predominately petrol fuelled fleet 20 years ago in Germany. The results show that despite an increase in the

https://doi.org/10.5194/acp-2019-1070
Preprint. Discussion started: 3 December 2019

number of diesel fuelled vehicles over the past two decades in Europe, and updated emissions control technologies, the $HONO/NO_x$ emission ratio has not varied significantly. A comparison with a tunnel study in Hong Kong suggested that the $HONO/NO_x$ ratio may be less dependent on the percentage of diesel vehicles but rather the percentage of large goods vehicles within the fleet, and the after-treatment technologies implemented on those vehicles.

The $HONO/NO_x$ emission ratio determined in this study was used to investigate the contribution of vehicle exhaust HONO to ambient HONO in Birmingham. The results show that direct vehicles emissions contribute up to 70% of the total measured HONO in the city centre. As direct HONO emissions were found to be the dominant source where traffic density is high, it is important to obtain fuel-based emission ratios which also take into account after-treatment technologies, to ensure models can accurately simulate daytime OH radical production rates.

In this study the focus has been primarily on diesel and petrol fuelled vehicle HONO emissions. However in countries where alternative fuels such as liquefied petroleum gas (LPG) and compressed natural gas (CNG) are becoming more prevalent, in particular in the public transport sector, further investigation into HONO emissions from these fuel types is needed.

Author contribution

Study conceived by WB, FP and SB. Measurements were performed by LK, LC, TA, SB and FP. Formal analysis performed by LK, TA and SB. LK prepared the manuscript with contributions from all co-authors.

Competing Interests

The authors declare that they have no conflict of interest.

Data Availability

Hourly averaged fuel type, vehicle type and emission ratios are available in the Supplementary Information. The 15 minute dataset from the tunnel measurements is available from the authors on request.

Acknowledgements

The authors would like to thank the staff from Amey for their help in accessing the measurement site. We would also like to thank Birmingham City Council for their input and provision of ANPR data. This work was funded by the Natural Environment Research Council (NERC), NE/M013545/1 (Sources of Nitrous Acid in the Atmospheric Boundary Layer). Researchers from the University of Leicester were funded by a grant from NERC NE/M010554/1 (also titled: Sources of Nitrous acid in the Atmospheric Boundary Layer).

https://doi.org/10.5194/acp-2019-1070
Preprint. Discussion started: 3 December 2019

Atmospheric Chemistry and Physics Discussions

References

Alicke, B., Platt, U. and Stutz, J.: Impact of nitrous acid photolysis on the total hydroxyl radical budget during the Limitation of Oxidant Production/Pianura Padana Produzione di Ozono study in Milan, J. Geophys. Res. Atmos., 107(22), doi:10.1029/2000JD000075, 2002.

Ammann, M., Kalberer, M., Jost, D. T., Tobler, L., Rössler, E., Piguet, D., Gäggeler, H. W. and Baltensperger, U.: Heterogeneous production of nitrous acid on soot in polluted air masses, Nature, 395(6698), 157–160, doi:10.1038/25965, 1998.

Arens, F., Gutzwiller, L., Baltensperger, U., Gäggeler, H. W. and Ammann, M.: Heterogeneous Reaction of NO_2 on Diesel Soot Particles, Environ. Sci. Technol., 35(11), 2191–2199, doi:10.1021/es000207s, 2001.

Aubin, D. G. and Abbatt, J. P. D.: Interaction of NO_2 with hydrocarbon soot: Focus on HONO yield, surface modification, and mechanism, J. Phys. Chem. A, 111(28), 6263–6273, doi:10.1021/jp068884h, 2007.

Calvert, J. G., Yarwood, G. and Dunker, A. M.: An evaluation of the mechanism of nitrous acid formation in the urban atmosphere, Res. Chem. Intermed., 20(3–5), 463–502, doi:10.1163/156856794X00423, 1994.

Crilley, L. R., Kramer, L., Pope, F. D., Whalley, L. K., Cryer, D. R., Heard, D. E., Lee, J. D., Reed, C. and Bloss, W. J.: On the interpretation of in situ HONO observations via photochemical steady state, Faraday Discuss., 189, doi:10.1039/c5fd00224a, 2016.

DEFRA: DEFRA, 2017: Emission Factors Toolkit for Vehicle Emissions., [online] Available from: https://laqm.defra.gov.uk/review-and-assessment/tools/emissions-factors-toolkit.html (Accessed 14 July 2019), 2017.

DfT: Vehicle licensing statistics: 2016, [online] Available from: https://www.gov.uk/government/statistics/vehicle-licensing-statistics-2016 (Accessed 26 April 2019), 2017.

Dunlea, E. J., Herndon, S. C., Nelson, D. D., Volkamer, R. M., San Martini, F., Sheehy, P. M., Zahniser, M. S., Shorter, J. H., Wormhoudt, J. C., Lamb, B. K., Allwine, E. J., Gaffney, J. S., Marley, N. A., Grutter, M., Marquez, C., Blanco, S., Cardenas, B., Retama, A., Yillegas, C. R. R., Kolb, C. E., Molina, L. T. and Molina, M. J.: Evaluation of nitrogen dioxide chemiluminescence monitors in a polluted urban environment, Atmos. Chem. Phys., 7(10), 2691–2704, doi:10.5194/acp-7-2691-2007, 2007.

Elshorbany, Y. F., Kurtenbach, R., Wiesen, P., Lissi, E., Rubio, M., Villena, G., Gramsch, E., Rickard, A. R., Pilling, M. J. and Kleffmann, J.: Oxidation capacity of the city air of Santiago, Chile, Atmos. Chem. Phys., 9(6), 2257–2273, doi:10.5194/acp-9-2257-2009, 2009.

Finlayson-Pitts, B. J., Wingen, L. M., Sumner, A. L., Syomin, D. and Ramazan, K. A.: The heterogeneous hydrolysis of NO_2 in laboratory systems and in outdoor and indoor atmospheres: An integrated mechanism, Phys. Chem. Chem. Phys., 5(2), 223–242, doi:10.1039/b208564j, 2003.

George, C., Strekowski, R. S., Kleffmann, J., Stemmler, K. and Ammann, M.: Photoenhanced uptake of gaseous NO_2 on solid organic compounds: A photochemical source of HONO?, Faraday Discuss., 130(2), 195–210, doi:10.1039/b417888m, 2005.

Gerecke, A., Thielmann, A., Gutzwiller, L. and Rossi, M. J.: The chemical kinetics of HONO formation resulting from heterogeneous interaction of NO_2 with flame soot, Geophys. Res. Lett., 25(13), 2453–2456, doi:10.1029/98GL01796, 1998.

Guan, C., Li, X., Zhang, W. and Huang, Z.: Identification of nitration products during heterogeneous reaction of NO_2 on soot in the dark and under simulated sunlight, J. Phys. Chem. A, 121(2), 482–492, doi:10.1021/acs.jpca.6b08982, 2017.

He, C., Li, J., Ma, Z., Tan, J. and Zhao, L.: High NO_2/NO_x emissions downstream of the catalytic diesel particulate filter: An influencing factor study, J. Environ. Sci. (China), 35(2), 55–61, doi:10.1016/j.jes.2015.02.009, 2015.

Ho, K. F., Sai Hang Ho, S., Cheng, Y., Lee, S. C. and Zhen Yu, J.: Real-world emission factors of fifteen carbonyl compounds measured in a Hong Kong tunnel, Atmos. Environ., 41(8), 1747–1758, doi:10.1016/j.atmosenv.2006.10.027, 2007.

https://doi.org/10.5194/acp-2019-1070
Preprint. Discussion started: 3 December 2019

Atmospheric Chemistry and Physics Discussions

Huang, R. J., Yang, L., Cao, J., Wang, Q., Tie, X., Ho, K. F., Shen, Z., Zhang, R., Li, G., Zhu, C., Zhang, N., Dai, W., Zhou, J., Liu, S., Chen, Y., Chen, J. and O'Dowd, C. D.: Concentration and sources of atmospheric nitrous acid (HONO) at an urban site in Western China, Sci. Total Environ., 593–594, 165–172, doi:10.1016/j.scitotenv.2017.02.166, 2017.

Jenkin, M. E., Cox, R. A. and Williams, D. J.: Laboratory studies of the kinetics of formation of nitrous acid from the thermal reaction of nitrogen dioxide and water vapour, Atmos. Environ., 22(3), 487–498, doi:10.1016/0004-6981(88)90194-1, 1988.

Kalberer, M., Ammann, M., Arens, F., Gäggeler, H. W. and Baltensperger, U.: Heterogeneous formation of nitrous acid (HONO) on soot aerosol particles, J. Geophys. Res. Atmos., 104(D11), 13825–13832, doi:10.1029/1999JD900141, 1999.

Khalizov, A. F., Cruz-Quinones, M. and Zhang, R.: Heterogeneous reaction of NO_2 on fresh and coated soot surfaces, J. Phys. Chem. A, 114(28), 7516–7524, doi:10.1021/jp1021938, 2010.

Kim, J. H., Kim, M. Y. and Kim, H. G.: NO_2-assisted sort regeneration behavior in a diesel particulate filter with heavy-duty diesel exhaust gases, Numer. Heat Transf. Part A Appl., 58(9), 725–739, doi:10.1080/10407782.2010.523293, 2010.

Kirchstetter, T. W., Harley, R. A. and Littlejohn, D.: Measurement of Nitrous Acid in Motor Vehicle Exhaust, Environ. Sci. Technol., 30(9), 2843–2849, doi:10.1021/es960135y, 1996.

Kirchstetter, T. W., Harley, R. A., Kreisberg, N. M., Stolzenburg, M. R. and Hering, S. V.: On-road measurement of fine particle and nitrogen oxide emissions from light- and heavy-duty motor vehicles, Atmos. Environ., 33(18), 2955–2968, doi:10.1016/S1352-2310(99)00089-8, 1999.

Kleffmann, J.: Daytime sources of nitrous acid (HONO) in the atmospheric boundary layer, ChemPhysChem, 8(8), 1137–1144, doi:10.1002/cphc.200700016, 2007.

Kleffmann, J., Becker, K. H. and Wiesen, P.: Heterogenous NO_2 Conversion Process on acid surfaces: Possible Atmospheric Implications, Atmos. Environ., 32(16), 2721–2729, doi:https://doi.org/10.1016/S1352-2310(98)00065-X, 1998.

Kleffmann, J., Becker, K. H., Lackhoff, M. and Wiesen, P.: Heterogeneous conversion of NO_2 on carbonaceous surfaces, Phys. Chem. Chem. Phys., 1(24), 5443–5450, doi:10.1039/a905545b, 1999.

Kurtenbach, R., Becker, K. H., Gomes, J. A. G., Kleffmann, J., Lörzer, J. C., Spittler, M., Wiesen, P., Ackermann, R., Geyer, A. and Platt, U.: Investigations of emissions and heterogeneous formation of HONO in a road traffic tunnel, Atmos. Environ., 35(20), 3385–3394, doi:10.1016/S1352-2310(01)00138-8, 2001.

Langridge, J. M., Gustafsson, R. J., Griffiths, P. T., Cox, R. A., Lambert, R. M. and Jones, R. L.: Solar driven nitrous acid formation on building material surfaces containing titanium dioxide: A concern for air quality in urban areas?, Atmos. Environ., 43(32), 5128–5131, doi:10.1016/j.atmosenv.2009.06.046, 2009.

Laufs, S., Cazaunau, M., Stella, P., Kurtenbach, R., Cellier, P., Mellouki, A., Loubet, B. and Kleffmann, J.: Diurnal fluxes of HONO above a crop rotation, Atmos. Chem. Phys., 17(11), 6907–6923, doi:10.5194/acp-17-6907-2017, 2017.

Lee, B. H., Wood, E. C., Herndon, S. C., Lefer, B. L., Luke, W. T., Brune, W. H., Nelson, D. D., Zahniser, M. S. and Munger, J. W.: Urban measurements of atmospheric nitrous acid: A caveat on the interpretation of the HONO photostationary state, J. Geophys. Res. Atmos., 118(21), 12274–12281, doi:10.1002/2013JD020341, 2013.

Lee, J. D., Whalley, L. K., Heard, D. E., Stone, D., Dunmore, R. E., Hamilton, J. F., Young, D. E., Allan, J. D., Laufs, S. and Kleffmann, J.: Detailed budget analysis of HONO in central London reveals a missing daytime source, Atmos. Chem. Phys., 16(5), 2747–2764, doi:10.5194/acp-16-2747-2016, 2016.

Lelièvre, S., Bedjanian, Y., Laverdet, G. and Le Bras, G.: Heterogeneous reaction of NO_2 with hydrocarbon flame soot, J. Phys. Chem. A, 108(49), 10807–10817, doi:10.1021/jp0469970, 2004.

Liang, Y., Zha, Q., Wang, W., Cui, L., Lui, K. H., Ho, K. F., Wang, Z., Lee, S. C. and Wang, T.: Revisiting nitrous acid (HONO) emission from on-road vehicles: A tunnel study with a mixed fleet, J. Air Waste Manag. Assoc., 67(7), 797–805, doi:10.1080/10962247.2017.1293573, 2017.

https://doi.org/10.5194/acp-2019-1070
Preprint. Discussion started: 3 December 2019

Liu, Y., Lu, K., Ma, Y., Yang, X., Zhang, W., Wu, Y., Peng, J., Shuai, S., Hu, M. and Zhang, Y.: Direct emission of nitrous acid (HONO) from gasoline cars in China determined by vehicle chassis dynamometer experiments, Atmos. Environ., 169, 89–96, doi:10.1016/j.atmosenv.2017.07.019, 2017.

Maier, S., Tamm, A., Wu, D., Caesar, J., Grube, M. and Weber, B.: Photoautotrophic organisms control microbial abundance, diversity, and physiology in different types of biological soil crusts, ISME J., 12(4), 1032–1046, doi:10.1038/s41396-018-0062-8, 2018.

Maljanen, M., Yli-Pirilä, P., Hytönen, J., Joutsensaari, J. and Martikainen, P. J.: Acidic northern soils as sources of atmospheric nitrous acid (HONO), Soil Biol. Biochem., 67(2), 94–97, doi:10.1016/j.soilbio.2013.08.013, 2013.

Meusel, H., Tamm, A., Kuhn, U., Wu, D., Lena Leifke, A., Fiedler, S., Ruckteschler, N., Yordanova, P., Lang-Yona, N., Pöhlker, M., Lelieveld, J., Hoffmann, T., Pöschl, U., Su, H., Weber, B. and Cheng, Y.: Emission of nitrous acid from soil and biological soil crusts represents an important source of HONO in the remote atmosphere in Cyprus, Atmos. Chem. Phys., 18(2), 799–813, doi:10.5194/acp-18-799-2018, 2018.

Michoud, V., Kukui, A., Camredon, M., Colomb, A., Borbon, A., Miet, K., Aumont, B., Beekmann, M., Durand-Jolibois, R., Perrier, S., Zapf, P., Siour, G., Ait-Helal, W., Locoge, N., Sauvage, S., Afif, C., Gros, V., Furger, M., Ancellet, G. and Doussin, J. F.: Radical budget analysis in a suburban European site during the MEGAPOLI summer field campaign, Atmos. Chem. Phys., 12(24), 11951–11974, doi:10.5194/acp-12-11951-2012, 2012.

Michoud, V., Colomb, A., Borbon, A., Miet, K., Beekmann, M., Camredon, M., Aumont, B., Perrier, S., Zapf, P., Siour, G., Ait-Helal, W., Afif, C., Kukui, A., Furger, M., Dupont, J. C., Haeffelin, M. and Doussin, J. F.: Study of the unknown HONO daytime source at a European suburban site during the MEGAPOLI summer and winter field campaigns, Atmos. Chem. Phys., 14(6), 2805–2822, doi:10.5194/acp-14-2805-2014, 2014.

Monge, M. E., D'Anna, B., Mazri, L., Giroir-Fendler, A., Ammann, M., Donaldson, D. J. and George, C.: Light changes the atmospheric reactivity of soot, Proc. Natl. Acad. Sci., 107(15), 6605–6609, doi:10.1073/pnas.0908341107, 2010.

Nakashima, Y. and Kajii, Y.: Determination of nitrous acid emission factors from a gasoline vehicle using a chassis dynamometer combined with incoherent broadband cavity-enhanced absorption spectroscopy, Sci. Total Environ., 575, 287–293, doi:10.1016/j.scitotenv.2016.10.050, 2017.

Ning, Z., Wubulihairen, M. and Yang, F.: PM, NO_x and butane emissions from on-road vehicle fleets in Hong Kong and their implications on emission control policy, Atmos. Environ., 61(2), 265–274, doi:10.1016/j.atmosenv.2012.07.047, 2012.

O'Driscoll, R., Stettler, M. E. J., Molden, N., Oxley, T. and ApSimon, H. M.: Real world CO_2 and NO_x emissions from 149 Euro 5 and 6 diesel, gasoline and hybrid passenger cars, Sci. Total Environ., 621(x), 282–290, doi:10.1016/j.scitotenv.2017.11.271, 2018.

Oswald, R., Behrendt, T., Ermel, M., Wu, D., Su, H., Cheng, Y., Breuninger, C., Moravek, A., Mougin, E., Delon, C., Loubet, B., Pommerening-Röser, A., Sörgel, M., Pöschl, U., Hoffmann, T., Andreae, M. O., Meixner, F. X. and Trebs, I.: HONO emissions from soil bacteria as a major source of atmospheric reactive nitrogen., Science, 341(6151), 1233–5, doi:10.1126/science.1242266, 2013.

Pierson, W. R., Brachaczek, W. W., Hammerle, R. H., McKee, D. E. and Butler, J. W.: Sulfate Emissions from Vehicles on the Road, J. Air Pollut. Control Assoc., 28(2), 123–132, doi:10.1080/00022470.1978.10470579, 1978.

Pierson, W. R., Gertler, A. W., Robinson, N. F., Sagebiel, J. C., Zielinska, B., Bishop, G. A., Stedman, D. H., Zweidinger, R. B. and Ray, W. D.: Real-world automotive emissions - summary of studies in the Fort McHenry and Tuscarora Mountain Tunnels, in Atmospheric Environment, vol. 30, pp. 2233–2256., 1996.

Pitts, J. N., Biermann, H. W., Winer, A. M. and Tuazon, E. C.: Spectroscopic identification and measurement of gaseous nitrous acid in dilute auto exhaust, Atmos. Environ., 18(4), 847–854, doi:10.1016/0004-6981(84)90270-1, 1984.

Qin, M., Xie, P., Su, H., Gu, J., Peng, F., Li, S., Zeng, L., Liu, J., Liu, W. and Zhang, Y.: An observational study of the HONO-NO_2 coupling at an urban site in Guangzhou City, South China, Atmos. Environ., 43(36), 5731–5742, doi:10.1016/j.atmosenv.2009.08.017, 2009.

Rappengluck, B., Lubertino, G., Alvarez, S., Golovko, J., Czader, B. and Ackermann, L.: Radical precursors and related species from traffic as observed and modeled at an urban highway junction, J Air Waste Manag Assoc, 63(11), 1270–1286, doi:10.1080/10962247.2013.822438,

2013.

Reed, C., Evans, M. J., Crilley, L. R., Bloss, W. J., Sherwen, T., Read, K. A., Lee, J. D. and Carpenter, L. J.: Evidence for renoxification in the tropical marine boundary layer, Atmos. Chem. Phys. Discuss., 1–29, doi:10.5194/acp-2016-1111, 2017.

Rhead, M., Gurney, R., Ramalingam, S. and Cohen, N.: Accuracy of automatic number plate recognition (ANPR) and real world UK number plate problems, Proc. - Int. Carnahan Conf. Secur. Technol., 286–291, doi:10.1109/CCST.2012.6393574, 2012.

Richard, C., Gordon, I. E., Rothman, L. S., Abel, M., Frommhold, L., Gustafsson, M., Hartmann, J. M., Hermans, C., Lafferty, W. J., Orton, G. S., Smith, K. M. and Tran, H.: New section of the HITRAN database: Collision-induced absorption (CIA), J. Quant. Spectrosc. Radiat. Transf., 113(11), 1276–1285, doi:10.1016/j.jqsrt.2011.11.004, 2012.

Rogak, S. N., Green, S. I. and Pott, U.: Use of tracer gas for direct calibration of emission-factor measurements in a traffic tunnel, J. Air Waste Manag. Assoc., 48(6), 545–552, doi:10.1080/10473289.1998.10463707, 1998.

Romanias, M. N., Bedjanian, Y., Zaras, A. M., Andrade-Eiroa, A., Shahla, R., Dagaut, P. and Philippidis, A.: Mineral oxides change the atmospheric reactivity of soot: NO_2 uptake under dark and UV irradiation conditions, J. Phys. Chem. A, 117(48), 12897–12911, doi:10.1021/jp407914f, 2013.

Sander, R.: Compilation of Henry's law constants (version 4.0) for water as solvent, Atmos. Chem. Phys., 15(8), 4399–4981, doi:10.5194/acp-15-4399-2015, 2015.

Singh, A.: Quantifying the effect of atmospheric pollution and meteorology on visibility and tropospheric chemistry, University of Birmingham. [online] Available from: https://etheses.bham.ac.uk//id/eprint/7828/, 2017.

Spataro, F. and Ianniello, A.: Sources of atmospheric nitrous acid: State of the science, current research needs, and future prospects, J. Air Waste Manage. Assoc., 64(11), 1232–1250, doi:10.1080/10962247.2014.952846, 2014.

Stadler, D. and Rossi, M. J.: The reactivity of NO_2 and HONO on flame soot at ambient temperature: The influence of combustion conditions, Phys. Chem. Chem. Phys., 2(23), 5420–5429, doi:10.1039/b005680o, 2000.

Stemmler, K., Ammann, M., Donders, C., Kleffmann, J. and George, C.: Photosensitized reduction of nitrogen dioxide on humic acid as a source of nitrous acid., Nature, 440(7081), 195–198, doi:10.1038/nature04603, 2006.

Stutz, J., Kim, E. S., Platt, U., Bruno, P., Perrino, C. and Febo, A.: UV-visible absorption cross sections of nitrous acid, J. Geophys. Res. Atmos., 105(D11), 14585–14592, doi:10.1029/2000JD900003, 2000.

Stutz, J., Alicke, B. and Neftel, A.: Nitrous acid formation in the urban atmosphere: Gradient measurements of NO_2 and HONO over grass in Milan, Italy, J. Geophys. Res., 107(D22), 8192, doi:10.1029/2001JD000390, 2002.

Stutz, J., Alicke, B., Ackermann, R., Geyer, A., Wang, S., White, A. B., Williams, E. J., Spicer, C. W. and Fast, J. D.: Relative humidity dependence of HONO chemistry in urban areas, J. Geophys. Res., 109(D3), D03307, doi:10.1029/2003JD004135, 2004.

Su, H., Cheng, Y., Oswald, R., Behrendt, T., Trebs, I., Meixner, F. X., Andreae, M. O., Cheng, P., Zhang, Y. and Pöschl, U.: Soil nitrite as a source of atmospheric HONO and OH radicals., Science, 333(6049), 1616–8, doi:10.1126/science.1207687, 2011.

Thalman, R., Baeza-Romero, M. T., Ball, S. M., Borrás, E., Daniels, M. J. S., Goodall, I. C. A., Henry, S. B., Karl, T., Keutsch, F. N., Kim, S., Mak, J., Monks, P. S., Muñoz, A., Orlando, J., Peppe, S., Rickard, A. R., Ródenas, M., Sánchez, P., Seco, R., Su, L., Tyndall, G., Vázquez, M., Vera, T., Waxman, E. and Volkamer, R.: Instrument intercomparison of glyoxal, methyl glyoxal and NO_2 under simulated atmospheric conditions, Atmos. Meas. Tech., 8(4), 1835–1862, doi:10.5194/amt-8-1835-2015, 2015.

Tong, S., Hou, S., Zhang, Y., Chu, B., Liu, Y., He, H., Zhao, P. and Ge, M.: Exploring the nitrous acid (HONO) formation mechanism in winter Beijing: Direct emissions and heterogeneous production in urban and suburban areas, Faraday Discuss., 189, 213–230, doi:10.1039/c5fd00163c, 2016.

Trinh, H. T., Imanishi, K., Morikawa, T., Hagino, H. and Takenaka, N.: Gaseous nitrous acid (HONO) and nitrogen oxides (NO_x) emission from gasoline and diesel vehicles under real-world driving test cycles, J. Air Waste Manag. Assoc., 67(4), 412–420,

doi:10.1080/10962247.2016.1240726, 2017.

Vandaele, A. C., Hermans, C., Simon, P. C., Carleer, M., Colin, R. and Coquartii, B.: Measurements of the NO_2 absorption cross-section from 42 000 cm−1 to 10 000 cm−1 (238–1000 nm) at 220 K and 294 K, J. Quant. Spectrosc. Radiat. Transf., 59(3), 171–184, 1998.

Vandenboer, T. C., Markovic, M. Z., Sanders, J. E., Ren, X., Pusede, S. E., Browne, E. C., Cohen, R. C., Zhang, L., Thomas, J., Brune, W. H. and Murphy, J. G.: Evidence for a nitrous acid (HONO) reservoir at the ground surface in Bakersfield, CA, during CalNex 2010, Jounal Geophys. Res., 119, 9093–9106, doi:10.1002/2013JD020971.Received, 2014.

Villena, G., Wiesen, P., Cantrell, C. A., Flocke, F., Fried, A., Hall, S. R., Hornbrook, R. S., Knapp, D., Kosciuch, E., Mauldin, R. L., McGrath, J. A., Montzka, D., Richter, D., Ullmann, K., Walega, J., Weibring, P., Weinheimer, A., Staebler, R. M., Liao, J., Huey, L. G. and Kleffmann, J.: Nitrous acid (HONO) during polar spring in Barrow, Alaska: A net source of OH radicals?, J. Geophys. Res. Atmos., 116(24), 1–12, doi:10.1029/2011JD016643, 2011.

Villena, G., Bejan, I., Kurtenbach, R., Wiesen, P. and Kleffmann, J.: Interferences of commercial NO2 instruments in the urban atmosphere and in a smog chamber, Atmos. Meas. Tech., 5(1), 149–159, doi:10.5194/amt-5-149-2012, 2012.

Vogel, B., Vogel, H., Kleffmann, J. and Kurtenbach, R.: Measured and simulated vertical profiles of nitrous acid - Part II. Model simulations and indications for a photolytic source, Atmos. Environ., 37(21), 2957–2966, doi:10.1016/S1352-2310(03)00243-7, 2003.

Wang, J., Zhang, X., Guo, J., Wang, Z. and Zhang, M.: Observation of nitrous acid (HONO) in Beijing, China: Seasonal variation, nocturnal formation and daytime budget, Sci. Total Environ., doi:10.1016/j.scitotenv.2017.02.159, 2017.

Wang, X., Ho, K. F., Chow, J. C., Kohl, S. D., Chan, C. S., Cui, L., Lee, S. cheng F., Chen, L. W. A., Ho, S. S. H., Cheng, Y. and Watson, J. G.: Hong Kong vehicle emission changes from 2003 to 2015 in the Shing Mun Tunnel, Aerosol Sci. Technol., 52(10), 1085–1098, doi:10.1080/02786826.2018.1456650, 2018.

Weber, B., Wu, D., Tamm, A., Ruckteschler, N., Rodríguez-Caballero, E., Steinkamp, J., Meusel, H., Elbert, W., Behrendt, T., Sörgel, M., Cheng, Y., Crutzen, P. J., Su, H. and Pöschl, U.: Biological soil crusts accelerate the nitrogen cycle through large NO and HONO emissions in drylands., Proc. Natl. Acad. Sci. U. S. A., 112(50), 15384–9, doi:10.1073/pnas.1515818112, 2015.

Xu, Z., Wang, T., Wu, J., Xue, L., Chan, J., Zha, Q., Zhou, S., Louie, P. K. K. and Luk, C. W. Y.: Nitrous acid (HONO) in a polluted subtropical atmosphere: Seasonal variability, direct vehicle emissions and heterogeneous production at ground surface, Atmos. Environ., 106(x), 100–109, doi:10.1016/j.atmosenv.2015.01.061, 2015.

Yang, Q., Su, H., Li, X., Cheng, Y., Lu, K., Cheng, P., Gu, J., Guo, S., Hu, M., Zeng, L., Zhu, T. and Zhang, Y.: Daytime HONO formation in the suburban area of the megacity Beijing, China, Sci. China Chem., 57(7), 1032–1042, doi:10.1007/s11426-013-5044-0, 2014.

Ye, C., Zhang, N., Gao, H. and Zhou, X.: Photolysis of Particulate Nitrate as a Source of HONO and NO_x, Environ. Sci. Technol., 51(12), 6849–6856, doi:10.1021/acs.est.7b00387, 2017.

Zhou, X., Zhang, N., Teravest, M., Tang, D., Hou, J., Bertman, S. and Stevens, P. S.: Nitric acid photolysis on forest canopy surface as a source for tropospheric nitrous acid, Nat. Geosci., 4(7), 440–443, doi:10.1038/ngeo1164, 2011.

https://doi.org/10.5194/acp-2019-1070
Preprint. Discussion started: 3 December 2019

Atmospheric Chemistry and Physics Discussions

Figures

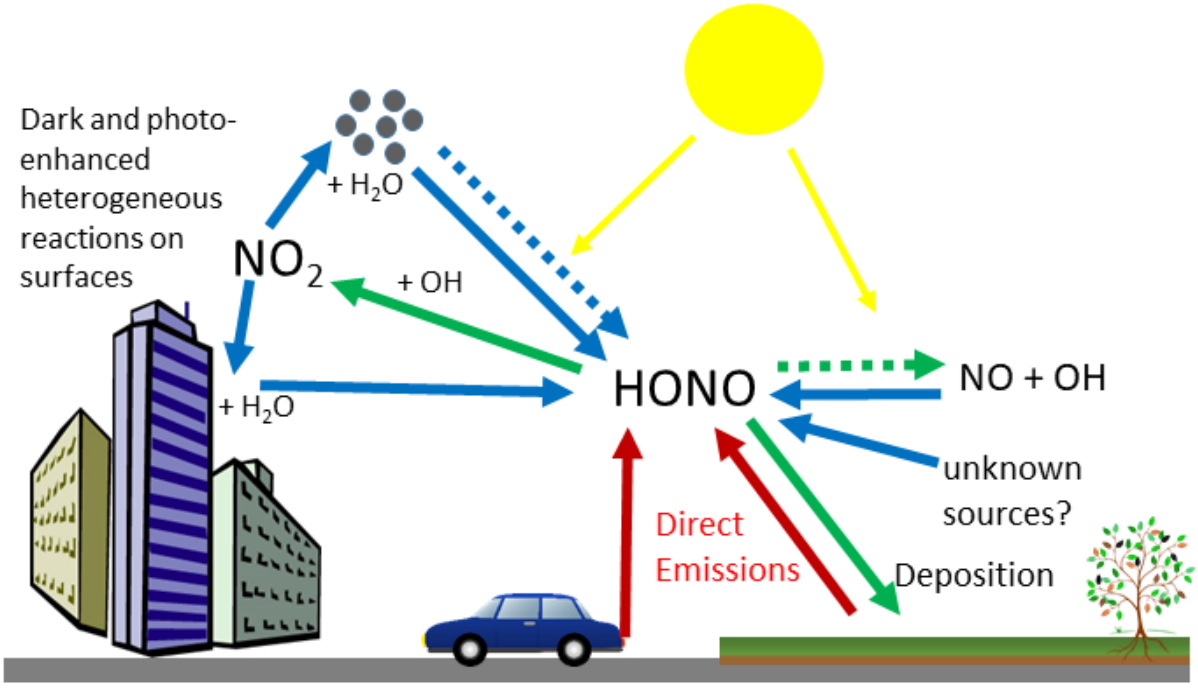

Figure 1: Sources and sinks of HONO in the troposphere, showing direct emission (red arrows), secondary sources (blue arrows) and HONO sinks (green arrows), dashed arrows represent solar driven reactions.

https://doi.org/10.5194/acp-2019-1070
Preprint. Discussion started: 3 December 2019

Atmospheric Chemistry and Physics Discussions

Figure 2: Map of Birmingham City Centre showing the M6 motorway (red dashed line) and schematic of the Queensway Tunnel (highlighted in blue on the map). © OpenStreetMap contributors 2019. Distributed under a Creative Commons BY-SA License.

https://doi.org/10.5194/acp-2019-1070
Preprint. Discussion started: 3 December 2019

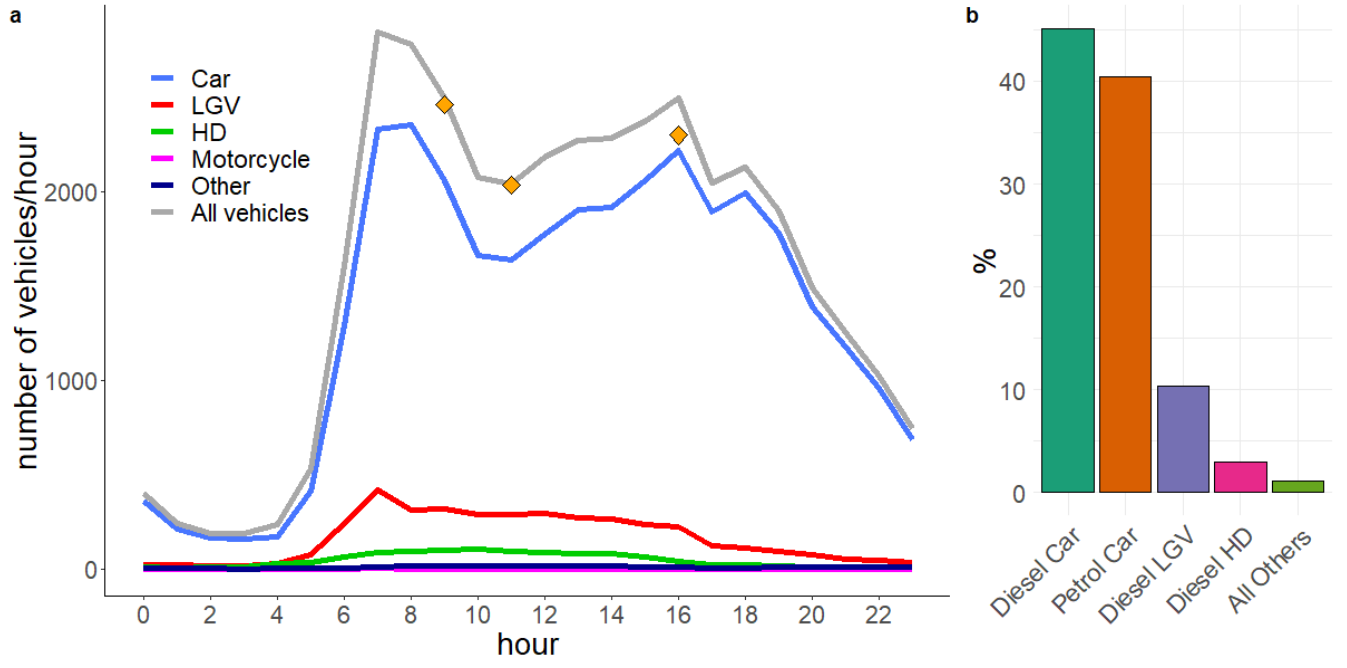

Figure 3: a) Average hourly vehicle fleet in the southbound tunnel from the corrected ANPR counts for weekdays (LGV = light goods vehicles, HD = heavy duty vehicles e.g. trucks, lorries and buses), orange points represent the counts estimated from video footage during the measurement period, b) percentage of vehicle types, determined from all weekday ANPR data in November 2016.

https://doi.org/10.5194/acp-2019-1070
Preprint. Discussion started: 3 December 2019

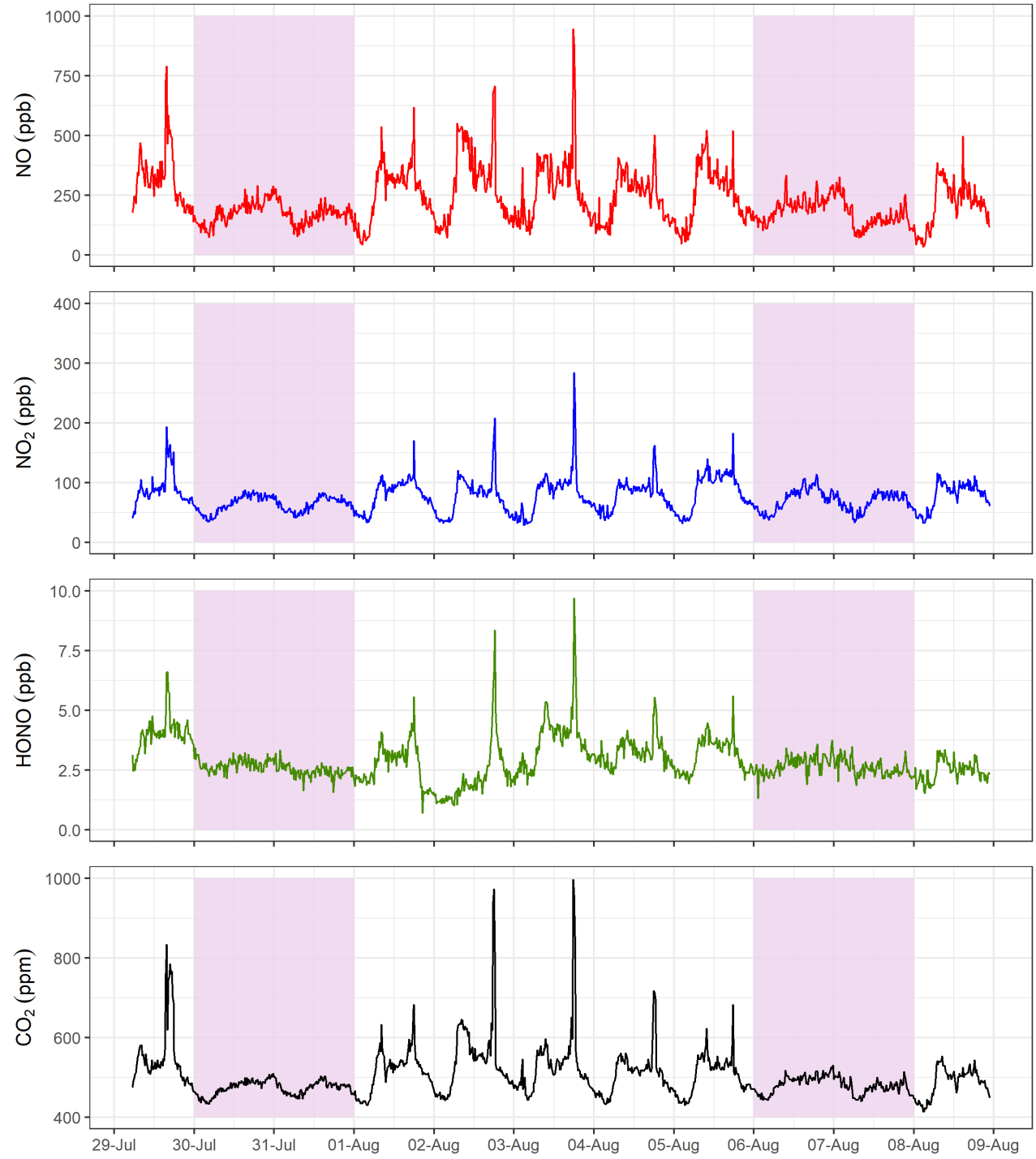

Figure 4: 15 minute averaged measurements of NO, NO_2, HONO and CO_2 from the Queensway tunnel between 29th July and 8th August 2016. Shaded areas indicate the weekends. Spikes in the measured mixing ratios on weekdays are the result of traffic congestion during morning and evening rush hour periods.

https://doi.org/10.5194/acp-2019-1070
Preprint. Discussion started: 3 December 2019

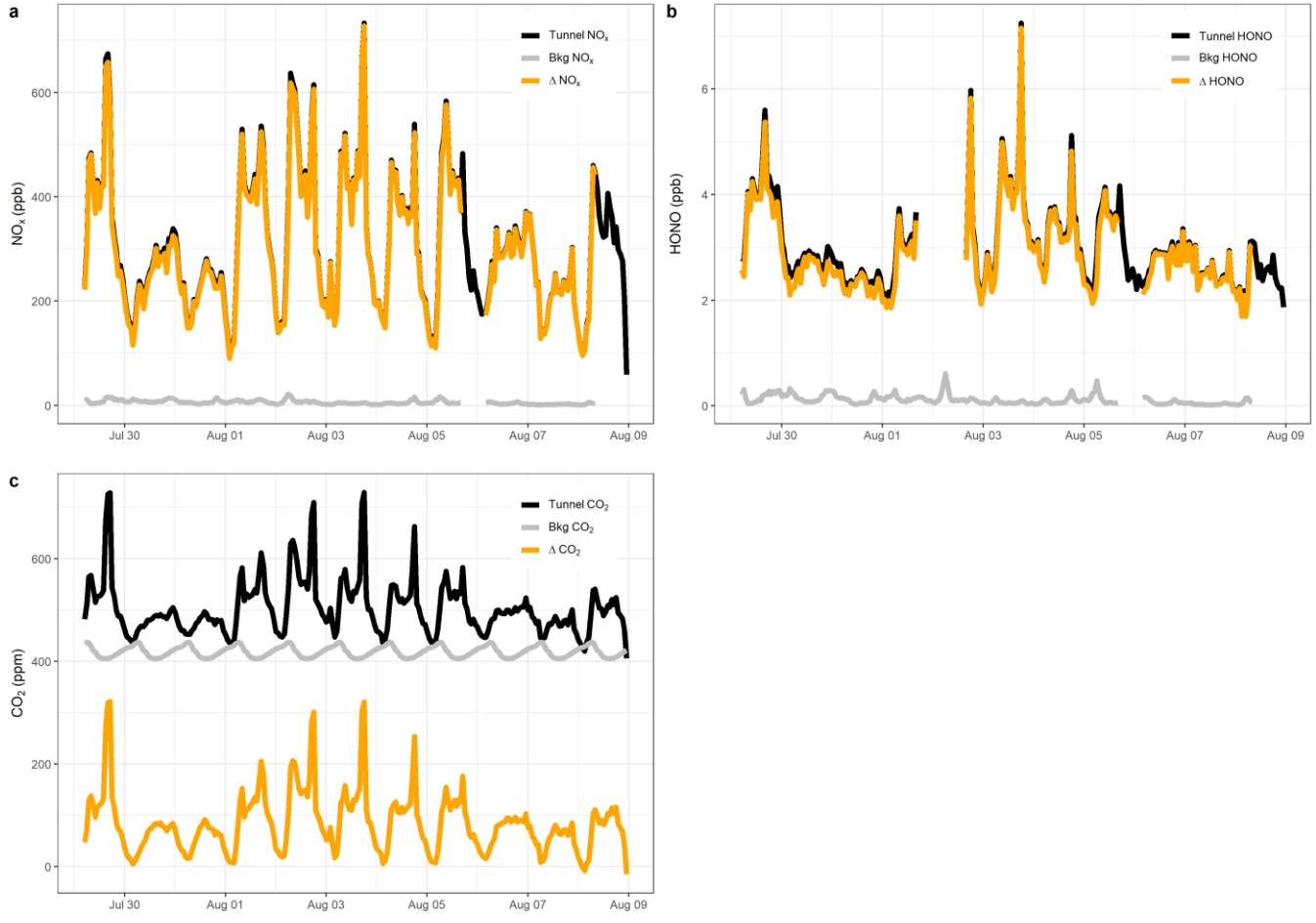

Figure 5: Hourly averaged time series a) NO_x in the tunnel and from Acocks Green urban background station, b) HONO in the tunnel and estimated background HONO, c) CO_2 in the tunnel and background CO_2 measured at BAQS.

https://doi.org/10.5194/acp-2019-1070
Preprint. Discussion started: 3 December 2019

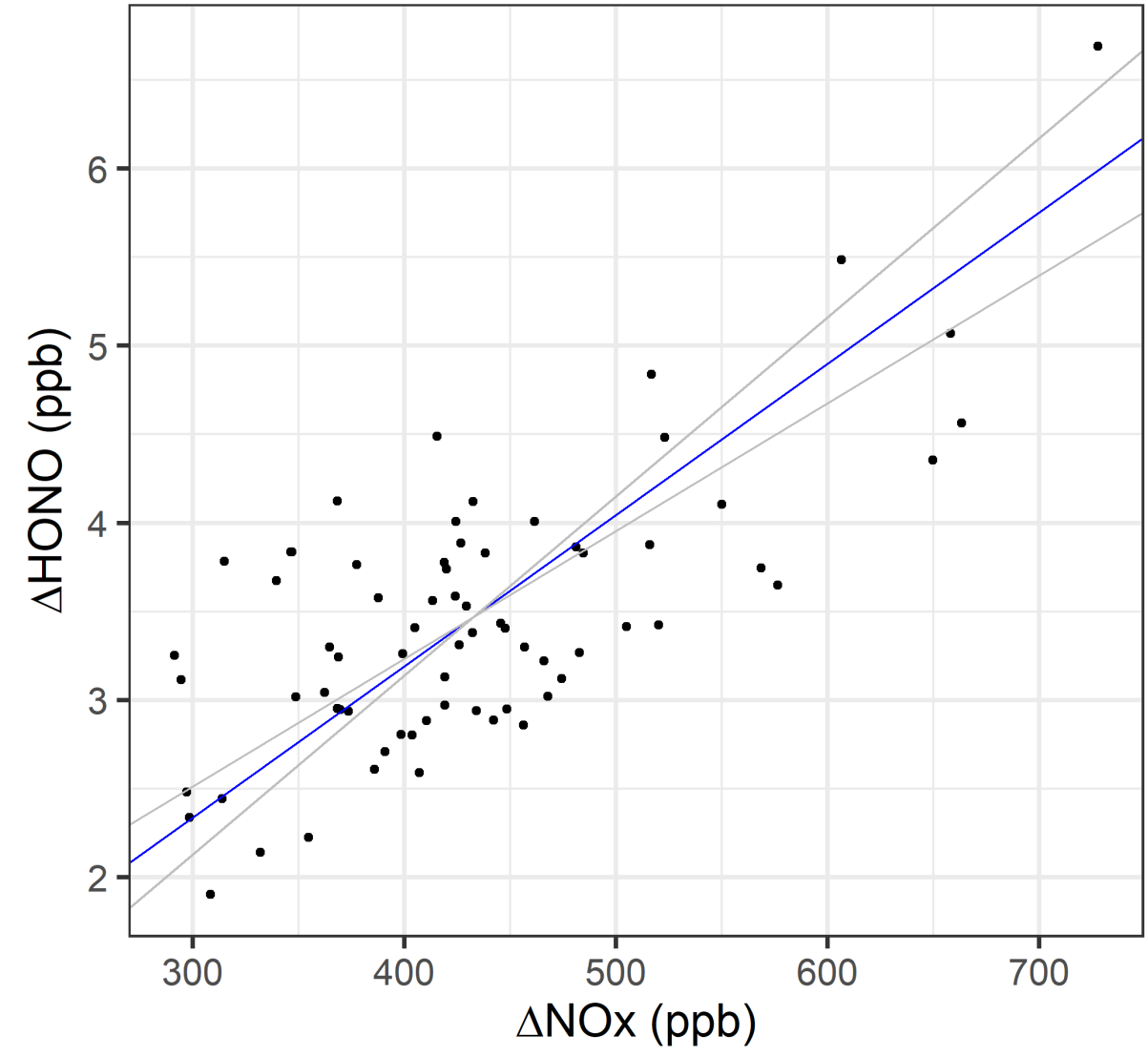

Figure 6: RMA regression for hourly averaged ΔNO_x versus ΔHONO, for weekdays between 06:00 and 19:00. The blue line represents the RMA slope and the grey lines the 95% confidence intervals of the regression.

https://doi.org/10.5194/acp-2019-1070
Preprint. Discussion started: 3 December 2019

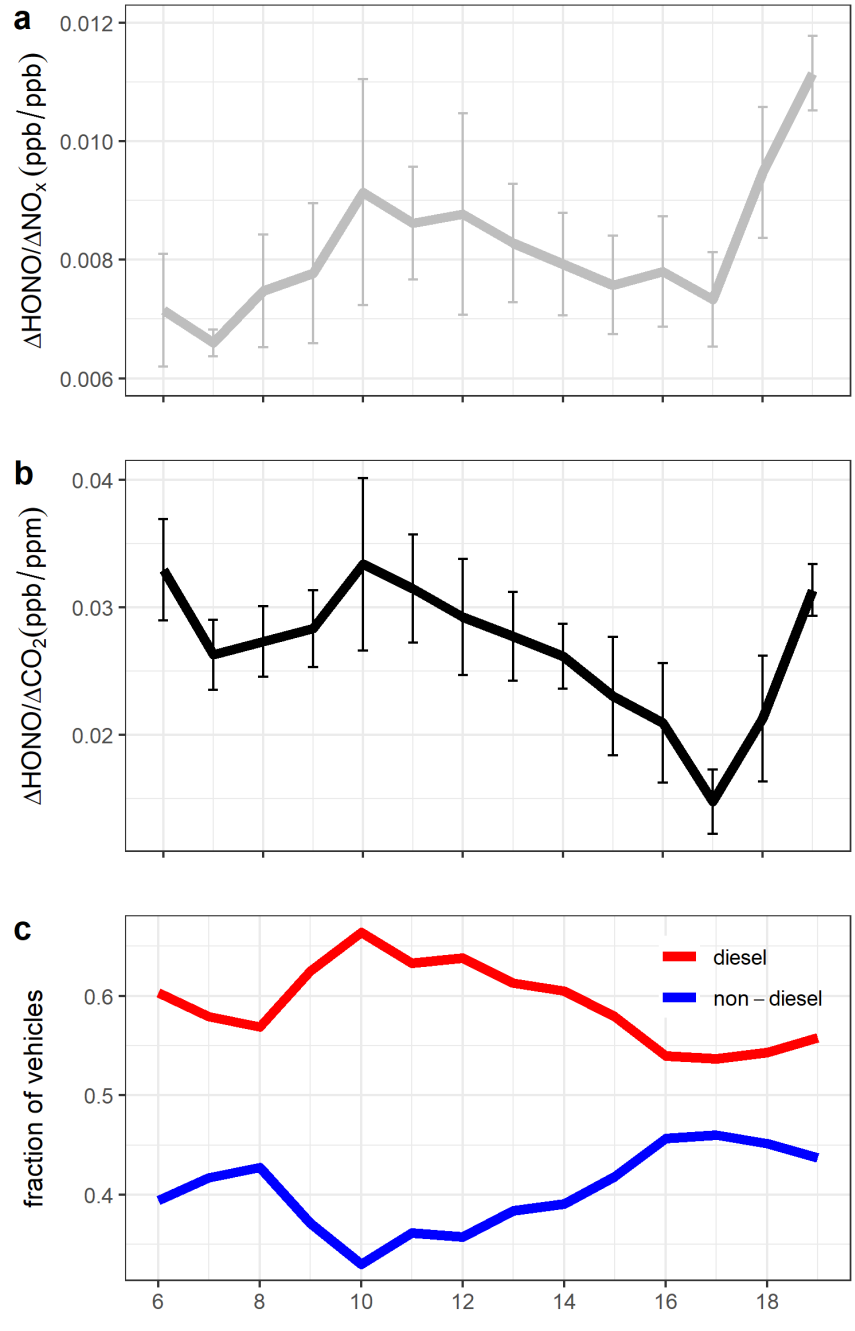

Figure 7: a) Hourly averaged ΔHONO/ΔNO$_x$ b) hourly averaged ΔHONO/ΔCO$_2$ and c) fraction of diesel and non-diesel (petrol, biofuel, electric) vehicles calculated from the total petrol and diesel vehicles, for the period between 06:00 and 19:00 during the weekday. Error bars represent 1-σ standard deviation of the mean across the different days of this study.

https://doi.org/10.5194/acp-2019-1070
Preprint. Discussion started: 3 December 2019

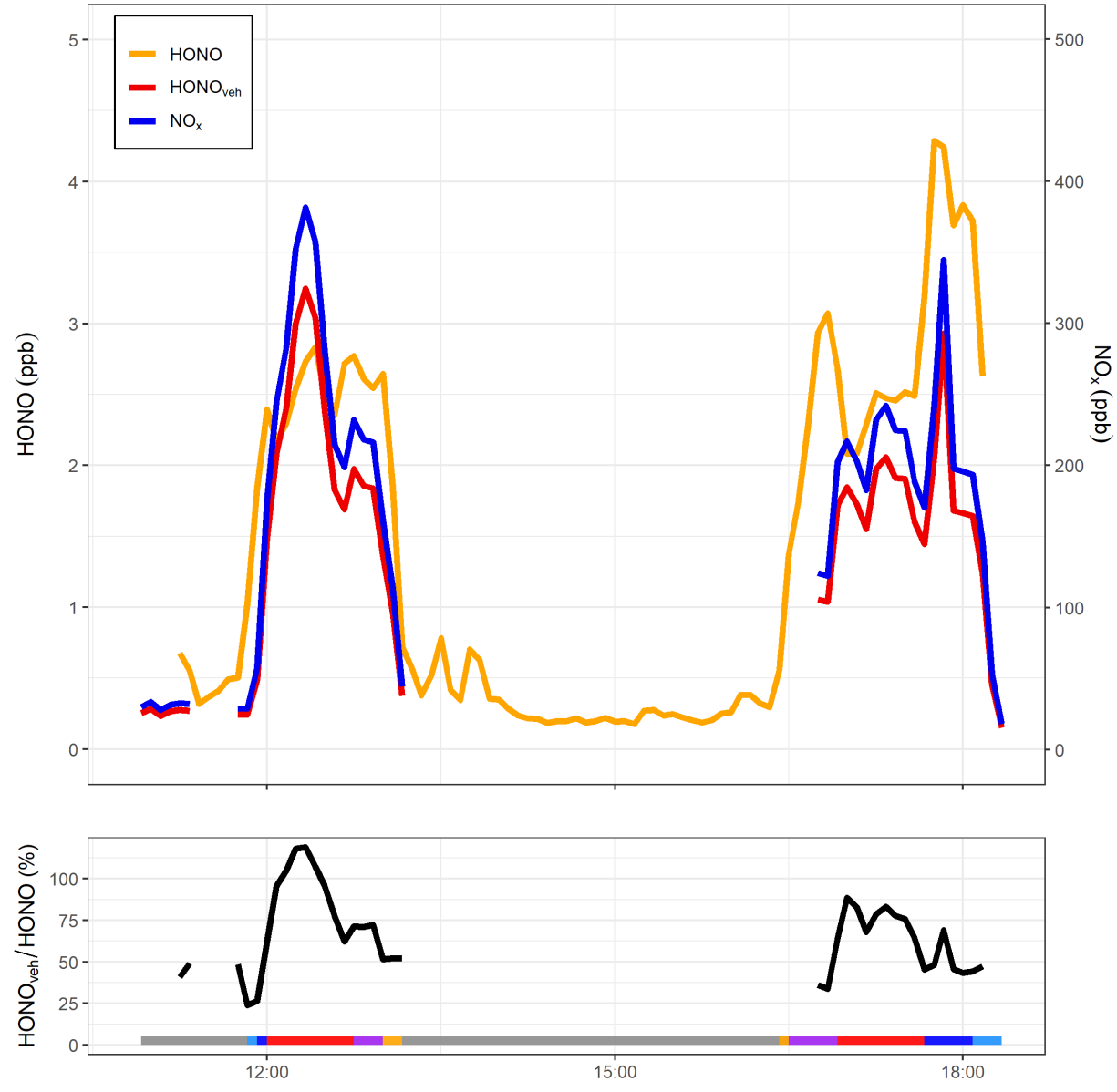

Figure 8: Top: NO_x, HONO and inferred vehicle exhaust HONO from mobile measurements taken on 23rd October 2015 along a transect between Birmingham and Leicester (Crilley et al. 2016). Bottom: ratio of $HONO_{veh}$/HONO (%) for the same period. Grey shaded areas represent non-driving periods, i.e. when the mobile laboratory was parked either at the University of Birmingham or University of Leicester campus. Other colours represent: measurements around the University of Birmingham campus (light blue), A38 road through Birmingham city centre (dark blue), M6/69 motorways (red), Leicester Ring Road (purple), and measurements around the University of Leicester campus (orange). $HONO_{veh}$/HONO above 100% are the result of uncertainties in the HONO and NO_x measurements and the HONO/NO_x ratio.

https://doi.org/10.5194/acp-2019-1070
Preprint. Discussion started: 3 December 2019

Atmospheric Chemistry and Physics Discussions

Tables

Table 1: Overview of instruments deployed in the Queensway Tunnel

Instrument	Measurement	Method	Sampling time (s)	Uncertainty
TEI: 42c	NO (and NO_y)	Chemiluminescence (Mo Conv.)	60	±10 %
BBCEAS (open-path)	HONO and NO_2	Broadband cavity enhanced absorption spectroscopy	20	5 ppbv (NO_2) 1.2 ppbv (HONO)
LICOR: LI-820	CO_2	non-dispersive infrared	1	± 5 %
Kestrel 4500: Mini-Met	Wind speed (WS), Temperature (T), Relative Humidity (RH)	-	600	-

Table 2: Comparison of HONO/NO_x ratios from different tunnel studies.

Location	Year of Study	Tunnel Length (m)	Avg. Vehicles /Day	Diesel Vehicles (%)	Petrol Vehicles (%)	Other (%)	HONO/NOx (%)	Reference
Queensway Tunnel Birmingham, U.K.	2016	548	37,700	59	40	<1	0.85 (CI:0.72-1.01)	This study
Shing Mun Tunnel Hong Kong	2015	1600	26,970	38	47	15[a]	1.24 ± 0.35	Liang et al., 2017
Kiesbergtunnel, Wuppertal, Germany	1997/ 1998	1100	22,000	24.3[b]	74.7	1	0.80 ± 0.10	Kurtenbach et al., 2001
Caldecott Tunnel California, U.S.	1995	1100	-	<0.2	99	-	0.29 ± 0.05	Kirchstetter et al. 1996

[a] LPG fuelled

[b] Includes LGVs and OGVs (assumption made here that these are diesel fuelled)